JOURNAL OF GUIDANCE, CONTROL, AND DYNAMICS
Vol. 33, No. 4, July–August 2010

Acceleration-Feedback-Enhanced Robust Control of an Unmanned Helicopter

Y. Q. He* and J. D. Han†
Chinese Academy of Sciences 110016 Shenyang, People's Republic of China

DOI: 10.2514/1.45659

While a few proposed control strategies have shown their acceptable effectiveness, performance improvement on stability and robustness of unmanned helicopters are still imperative and a great challenge due to strong nonlinearities, extensive parameter uncertainties and external disturbances when the flight condition is terrible, such as flight on a windy day. Because acceleration feedback control is advantageous in terms of simple controller structure and easy implementation, we attempt to incorporate it into the tracking control of an unmanned helicopter that is highly nonlinear and underactuated. In this paper, we use a prefilter to formulate a new acceleration feedback control and then use it as a robust enhancement for the H_∞ algorithm to attenuate uncertainties and external disturbances involved in the tracking control of an unmanned helicopter. We conduct simulations with an unmanned model helicopter and compare the tracking performance of the helicopter with and without acceleration feedback control. The results show that the use of acceleration feedback control does enhance tracking performance greatly compared to the standard H_∞ control.

Nomenclature

A, B, C, D	=	system matrix of linearization models
a_M, a_T	=	slope of lift curve of main and tail rotors, 1/rad
a_{1s}	=	longitudinal flapping angle of main rotor, rad
b_M, b_T	=	number of blade of main and tail rotors
b_{1s}	=	lateral flapping angle of main rotor, rad
c_{dM}, c_{dT}	=	drag coefficient of blade of main and tail rotors, N/rad
c_M, c_T	=	rotor width of main and tail rotors, m
$\boldsymbol{d}_{i,j}$	=	column vector, element of system matrix D
$\boldsymbol{e}_1$	=	position tracking error, m
e_2	=	yaw angle tracking error, rad
$\boldsymbol{e}_3, \boldsymbol{e}_4$	=	state variables of position tracking error dynamics
$\boldsymbol{F}_c$	=	forces produced by main and tail rotors, N
$\boldsymbol{F}_{\text{ext}}$	=	external forces exerting on the body of helicopter, N
g	=	acceleration due to gravity, m/s^2
h_*	=	vertical distance between the c.g. location and the acting point of several forces, m
I_b	=	aircraft moment of inertia, kg · m^2
K, K_1, K_2	=	H_∞ control gain matrix
$\boldsymbol{k_i}$	=	$\bar{n} \times \bar{n}$ matrix, elements of control gain matrix K
k_i	=	parameters to be designed for the filter in acceleration feedback control
l_*	=	longitudinal distance between the c.g. location and the acting point of several forces, m
L_i, M_i, N_i	=	moment exerting on the ith component of helicopter, N · m
L^s, M^s, N^s	=	simplified moment exerting on the body of helicopter, N · m
$\boldsymbol{M}_c$	=	moments produced by main and tail rotors, N
$\boldsymbol{M}_{\text{ext}}$	=	external moments exerting on the body of helicopter, N · m
m	=	helicopter total mass, kg
$\bar{m}$	=	number of input of the unified linearization model
$m_{iT}, m_{iM}, n_{jT}, n_{jM}$	=	temporary variables used in computing aerodynamics of main and tail rotors
n	=	number of element for the state variables x in the unified linearization model
$\bar{n}$	=	number of the subvector in the unified linearization system's state vector
P	=	positive definite matrix used in H_∞ controller
p	=	roll rate, rad/s
$\boldsymbol{p}, x, y, z$	=	$\boldsymbol{p}$ is position vector of helicopter, x, y and z are its projection on x, y and z axis of body coordination, m
$\boldsymbol{p}_d$	=	desired position vector, m
Q_M, Q_T	=	torque of main and tail rotors, N · m
Q_M^s, Q_T^s	=	simplified moment produced by main and tail rotors, N · m
q	=	pitch rate, rad/ sec
R	=	transformation matrix from body coordinate to the inertial frame
R_{0M}, R_{0T}	=	inner radius of main and tail rotors, m
R_{1M}, R_{1T}	=	radius of main and tail rotors, m
r	=	yaw rate, rad/ sec
S_*	=	simplified aerodynamics parameters
T_M, T_T	=	thrust of main and tail rotors, N
T_M^s, T_T^s	=	simplified thrust produced by main and tail rotors, N
V_c	=	vertical climb velocity of a helicopter, m/s
$\boldsymbol{v}, \boldsymbol{v}_1, v_2$	=	input vector of the feedback linearization model
$\tilde{\boldsymbol{v}}, \tilde{\boldsymbol{v}}_1, \tilde{v}_2$	=	output vector of acceleration feedback controller
W	=	temporary matrix used in computing H_∞ control through linear matrix inequalities
X	=	temporary matrix used in computing H_∞ control through linear matrix inequalities
X_i, Y_i, Z_i	=	body force in x, y, and z directions exerting on i component, N
$\boldsymbol{x}$	=	state variables of unified form of helicopter's linearization model
$\boldsymbol{y}$	=	outputs of unified form of helicopter's linearization model
y_M	=	lateral distance between the c.g. location and the acting point of a force, m
$\gamma, \gamma_1, \gamma_2$	=	input-output finite L_2 gain value
$\boldsymbol{\Delta}_F$,	=	force disturbances exerting on the body of the helicopter, $[\,\Delta_{F_X} \quad \Delta_{F_Y} \quad \Delta_{F_Z}\,]^T$, N

Received 27 May 2009; revision received 4 March 2010; accepted for publication 6 March 2010.

*Ph.D., State Key Laboratory of Robotics, Shenyang Institute of Automation; heyuqing@sia.cn.

†Professor, State Key Laboratory of Robotics, Shenyang Institute of Automation; jdhan@sia.cn.

$\bar{\boldsymbol{\Delta}}_F$	=	force disturbances exerting on the body of the helicopter, $[\,\bar{\Delta}_{F_X} \quad \bar{\Delta}_{F_Y} \quad \bar{\Delta}_{F_Z}\,]^T$, N
$\boldsymbol{\Delta}_M$,	=	moment disturbances exerting on the body of the helicopter, $[\,\Delta_{M_L} \quad \Delta_{M_M} \quad \Delta_{M_N}\,]^T$, $\mathrm{N \cdot m}$
$\bar{\boldsymbol{\Delta}}_M$	=	moment disturbances exerting on the body of the helicopter, $[\,\bar{\Delta}_{M_L} \quad \bar{\Delta}_{M_M} \quad \bar{\Delta}_{M_N}\,]^T$, $\mathrm{N \cdot m}$
$\boldsymbol{\Delta}_1$, $\boldsymbol{\Delta}_2$, Δ_3	=	gross disturbances exerting on the body of helicopters
$\boldsymbol{\delta}_F$	=	uncertainties term in position dynamics due to the simplification of aerodynamics, N
$\boldsymbol{\delta}_1$	=	gross uncertainties in position dynamics, N
$\tilde{\boldsymbol{\delta}}_1$	=	temporarily defined uncertainties term in position dynamics, N
$\boldsymbol{\delta}_2$	=	uncertainties due to the simplification of T_M, N
$\boldsymbol{\delta}_3$	=	uncertainties due to the simplification of M_c, $\mathrm{N \cdot m}$
$\tilde{\Delta}_1$, $\tilde{\Delta}_2$, $\tilde{\Delta}_3$	=	temporary defined disturbances during simplifying the dynamics
Θ	=	temporary variables used in acceleration feedback controller, $[\,\xi_1 \quad \xi_2 \quad \xi_3 \quad \cdots \quad \xi_m\,]^T$
θ	=	pitch angle, rad
θ_{c_M}, θ_{c_T}	=	collective pitch of main and tail rotors, rad
ρ	=	air density, $\mathrm{kg/m^3}$
σ, σ_1, σ_2	=	parameter in inequalities which uncertainty terms satisfy
Υ	=	temporary variable during computing the uncertainty
ψ	=	yaw angle, rad
ψ_d	=	desired yaw angle, rad
ϕ	=	roll angle, rad
Ω_M, Ω_T	=	angular velocity of the rotor, rpm
$\boldsymbol{\omega}$	=	angular velocity vector, rad/s
$\hat{\omega}$	=	Lie algebra isomorphism of ω, rad/s

Subscripts

M	=	main rotor
T	=	tail rotor
H	=	horizontal stabilizer
V	=	vertical stabilizer
F	=	fuselage
Δ	=	external disturbance

I. Introduction

TRAJECTORY tracking has been one of the most challenging problems in control of an unmanned helicopter due to the following facts discussed in [1–3]:

1) The dynamic model of an unmanned helicopter is strongly nonlinear, inherently unstable, and highly coupled.

2) The model may be a nonminimum phase system that has multiple inputs and multiple outputs (MIMO) and involves time-varying parameters.

3) The tracking control of an unmanned helicopter is influenced by external disturbances, such as the turbulence from tail rotor and lateral wind.

4) An unmanned helicopter system often needs to work in different flight modes, such as hovering, forward, backward, sideslip, upward and downward flights, and the dynamics is significantly different from one flight mode to another.

5) Most unmanned helicopters have four independent control inputs for its motion in six degrees of freedom (DOF), which forms an underactuated system.

While the classical techniques, most of which are based on dividing the system dynamics into several independent single-input/single-output (SISO) subsystems, may be applied into the autonomous control of an unmanned helicopter, there exists a so-called conservatism problem [4] due to the strong dynamics coupling. As a result, the autonomy of an unmanned helicopter may be restricted, especially when flying on a windy day and/or a complicated flight maneuver is demanded.

However, when performing dangerous and complicated tasks, such as disaster rescue in city area, unmanned helicopters should be highly stable and possess good tracking performance, which are far beyond what many controllers using classical SISO control strategy can achieve. This leads to a growing interest in applying nonlinear control methodology into the control of helicopters. Feedback linearization and state-dependent Riccati equation method [1,5], for example, were used to handle the nonlinear dynamics of a helicopter by online linearization and optimization. Backstepping and predictive control approaches have also been proposed for the control of helicopters [3,6,7], but the implementation of these methods is constrained due to the computational complexity and the lack of robustness [8]. Robust control such as H_∞ control [9,10], on the other hand, is well known for handling uncertainties and disturbances, but difficult to achieve a balance between robustness and conservation, since the uncertainty is usually supposed unknown. This problem is especially important when the uncertainties become large or time-varying.

Recently, the acceleration feedback control (AFC) has been successful in suppressing uncertainties and external disturbances of mechatronic systems [11–14]. There disturbances and uncertainties are presented as force or torque, which is directly reflected in acceleration signal. The AFC is advantageous in terms of simple controller structure and easy implementation and consequently has the potential to be applied to the control of an unmanned helicopter.

Before the AFC can be used in an unmanned helicopter, the acceleration signal needs to be made available. The acceleration in the study involves both linear and angular acceleration, which are obtainable in a real helicopter. The former can be easily measured by using a linear accelerometer, and the later can be measured directly using angular accelerometer, such as the piezoelectric angular accelerator [15] or using a number of linear accelerometers [16]. Moreover, angular acceleration can also be estimated [11].

There is certainly noise associated with the acceleration signal that needs to be sorted out. In our early work [17], in which the robust control was used as an inner-loop SISO controller of unmanned helicopter system, the noise in acceleration signals was attenuated using two different methods: passive method and active method. With the passive method, the acceleration sensors are isolated from the main body of helicopter by an isolator mounted inside the main avionics box. For the active method, some filter, such as a Kalman filter, can be used as verified experimentally [11,17]. Consequently, it is possible to obtain clean and effective acceleration signals.

While AFC has been successful [11–14], it cannot be used directly in the control of an unmanned helicopter for the following reasons:

1) The existing AFC algorithm requires a high-gain that is difficult to realize in a helicopter.

2) The existing AFC strategy cannot deal with an underactuated system such as a helicopter.

In this paper, AFC is revised to enhance the H_∞ algorithm to attenuate uncertainties and external disturbances involved in the tracking control of an unmanned helicopter. First, a helicopter dynamic model is formulated in such a way that it can be

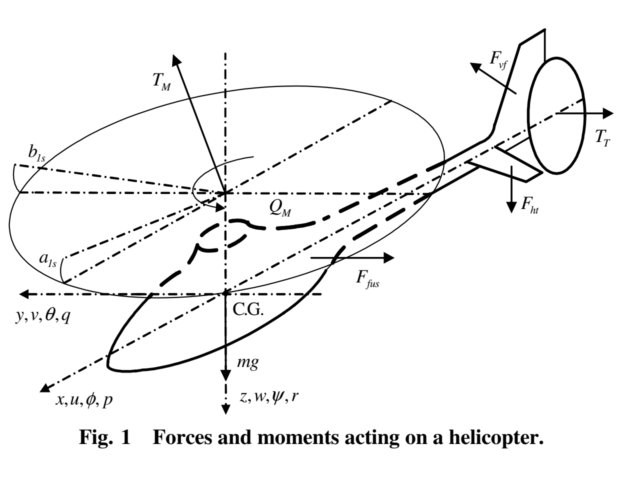

Fig. 1 Forces and moments acting on a helicopter.

feedback-linearized. Second, a nonlinear H_∞ control is designed based on the model to ensure the closed-loop stability and robustness with respect to external disturbances. Third, a revised AFC is used to further compensate uncertainties and reduce the conservatism of the H_∞ control. Finally, simulations are conducted on an unmanned model helicopter and the improvements of the tracking performance due to the use of the AFC are analyzed.

II. Dynamics of an Unmanned Helicopter

The dynamics of an unmanned helicopter system can be modeled as a 6-DOF rigid body with external forces and moments acting at the main and tail rotors, empennage and fuselage drag, as shown in Fig. 1 ([4], page 29). The motion of the helicopter is described in a coordinate system that is attached rigidly on the helicopter body with the origin being placed at the center of mass: x, y, and z axes pointing to the nose of airframe, right side, and downward, respectively. The motion dynamics is given as

$$\ddot{\boldsymbol{p}} = [0 \quad 0 \quad g]^T + \frac{1}{m} R \boldsymbol{F}_{\mathrm{ext}} \qquad \dot{R} = R\hat{\omega}$$
$$\dot{\boldsymbol{\omega}} = I_b^{-1}(\boldsymbol{M}_{\mathrm{ext}} - \boldsymbol{\omega} \times I_b \boldsymbol{\omega}) \tag{1}$$

where $\boldsymbol{p} = [x, y, z]^T$ is the positional vector, $\boldsymbol{\omega} = [p, q, r]^T$ is the angular velocity vector, and

$$\boldsymbol{F}_{\mathrm{ext}} = \begin{bmatrix} X \\ Y \\ Z \end{bmatrix} \quad \boldsymbol{M}_{\mathrm{ext}} = \begin{bmatrix} L \\ M \\ N \end{bmatrix} \quad \hat{\omega} = \begin{bmatrix} 0 & -r & q \\ r & 0 & -p \\ -q & p & 0 \end{bmatrix} \quad R = \begin{bmatrix} \cos\theta\cos\psi & \sin\phi\sin\theta\cos\psi - \cos\phi\sin\psi & \cos\phi\sin\theta\cos\psi + \sin\phi\sin\psi \\ \cos\theta\sin\psi & \sin\phi\sin\theta\sin\psi + \cos\phi\cos\psi & \cos\phi\sin\theta\sin\psi - \sin\phi\cos\psi \\ -\sin\theta & \sin\phi\cos\theta & \cos\phi\cos\theta \end{bmatrix}$$

where $\boldsymbol{F}_{\mathrm{ext}}$ and $\boldsymbol{M}_{\mathrm{ext}}$ are the sum of the external forces and moments acting on the airframe and are determined by

$$\begin{aligned} X &= X_M + X_T + X_H + X_V + X_F + X_\Delta \\ Y &= Y_M + Y_T + Y_V + Y_F + Y_\Delta \\ Z &= Z_M + Z_T + Z_H + Z_V + Z_F + Z_\Delta \\ L &= L_M + Y_M h_M + Z_M y_M + Y_T h_T + Y_V h_V \\ &\quad + Y_F h_F + L_F + L_\Delta \\ M &= M_M + M_T - X_M h_M + Z_M l_M - X_T h_T \\ &\quad + Z_T h_T - X_H h_H + Z_H l_H - X_V h_V + M_F + M_\Delta \\ N &= N_M - Y_M l_M - Y_T l_T - Y_V l_V + N_F - Y_F l_F + N_\Delta \end{aligned} \tag{2}$$

where X, Y, Z, and L, M, N are, respectively, the forces and moments exerting on the body of helicopter; both l_* and h_* represent the corresponding distances (Fig. 2); and the subscripts M, T, H, V, F, and Δ denote main rotor, tail rotor, horizontal stabilizer, vertical stabilizer, fuselage, and disturbance, respectively.

The force and moment generated by horizontal stabilizer, vertical fin, fuselage, and external disturbances are difficult to model. However, they can be neglected because their impact is relatively small. Consequently, the external forces and moments can be expressed as

$$\begin{aligned} X &= X_M + \Delta_{F_X}, \quad L = L_M + Y_M h_M + Z_M y_M + Y_T h_T + \Delta_{M_L} \\ Y &= Y_M + Y_T + \Delta_{F_Y}, \quad M = M_M + M_T - X_M h_M + Z_M l_M + \Delta_{M_M} \\ Z &= Z_M + \Delta_{F_Z} \quad N = N_M - Y_M l_M - Y_T l_T + \Delta_{M_N} \end{aligned} \tag{3}$$

And Eq. (1) can be rewritten as

$$\ddot{\boldsymbol{p}} = [0 \quad 0 \quad g]^T + \frac{1}{m} R \boldsymbol{F}_c + \bar{\boldsymbol{\Delta}}_F \qquad \dot{R} = R\hat{\omega}$$
$$\dot{\boldsymbol{\omega}} = I_b^{-1}(\boldsymbol{M}_c - \boldsymbol{\omega} \times I_b \boldsymbol{\omega}) + \bar{\boldsymbol{\Delta}}_M \tag{4}$$

where

$$\begin{aligned} \boldsymbol{F}_c &= \boldsymbol{F}_{\mathrm{ext}} - [\Delta_{F_X} \quad \Delta_{F_Y} \quad \Delta_{F_Z}]^T = [X_M \quad Y_M + Y_T \quad Z_M]^T \\ \boldsymbol{M}_c &= \boldsymbol{M}_{\mathrm{ext}} - [\Delta_{M_L} \quad \Delta_{M_M} \quad \Delta_{M_N}]^T = [L_M + Y_M h_M + Z_M y_M + Y_T h_T \quad M_M + M_T - X_M h_M + Z_M l_M \quad N_M - Y_M l_M - Y_T l_T]^T \\ \bar{\boldsymbol{\Delta}}_F &= \frac{1}{m} R [\Delta_{F_X} \quad \Delta_{F_Y} \quad \Delta_{F_Z}]^T \qquad \bar{\boldsymbol{\Delta}}_M = I_b^{-1} [\Delta_{M_L} \quad \Delta_{M_M} \quad \Delta_{M_N}]^T \end{aligned} \tag{5}$$

As the forces and moments generated by the main and tail rotors are controlled by T_M, T_T, a_{1s}, and b_{1s}, we obtain

$$\begin{aligned} X_M &= -T_M \sin a_{1s} \qquad L_M = -\left(\frac{\partial L_M}{\partial b_{1s}}\right) b_{1s} - Q_M \sin a_{1s} \\ Y_M &= T_M \sin b_{1s} \qquad M_M = \left(\frac{\partial M_M}{\partial a_{1s}}\right) a_{1s} - Q_M \sin b_{1s} \\ Z_M &= -T_M \cos a_{1s} \cos b_{1s} \qquad N_M = -Q_M \cos a_{1s} \cos b_{1s} \\ Y_T &= -T_T \qquad M_T = -Q_T \end{aligned} \tag{6}$$

where T_M and T_T are the forces exerting on the main rotor and tail rotor, and a_{1s} and b_{1s} stand for the longitudinal and lateral flapping angle of main rotor. Furthermore, the forces T_M and T_T and the moments Q_M and Q_T can be calculated as

$$\begin{aligned} T_i &= \frac{R_{1i}^3 - R_{0i}^3}{3} m_{3i}\theta_{ci} + \frac{m_{3i} m_{6i}}{2} (R_{1i}^2 - R_{0i}^2) - \frac{m_{3i}}{8\pi\Omega_i^2} \\ &\quad \times \left\{ \frac{2}{15 m_{2i}^2 \theta_{ci}^2} [(3m_{2i} R_{1i}\theta_{ci} - 2m_{5i}) \times (m_{2i} R_{1i}\theta_{ci} + m_{5i})^{3/2} \right. \\ &\quad \left. - (3m_{2i} R_{0i}\theta_{ci} - 2m_{5i})(m_{2i} R_{0i}\theta_{ci} + m_{5i})^{3/2}] \right\} \end{aligned} \tag{7}$$

$$\begin{aligned} Q_i &= n_{1i} n_{7i} \frac{R_{1i}^3 - R_{0i}^3}{3} - \frac{n_{1i} n_{9i}}{2} (R_{1i}^3 - R_{0i}^3) + \frac{c_{di} n_{1i}}{4} (R_{1i}^4 - R_{0i}^4) \\ &\quad + \frac{2 n_{1i} n_{8i}}{105 m_{4i}^3} \{ (15 m_{4i}^2 R_{1i}^2 - 12 m_{4i} m_{5i} R_{1i} + 8 m_{5i}^2)(m_{4i} R_{1i} \\ &\quad + m_{5i})^{3/2} - (15 m_{4i}^2 R_{0i}^2 - 12 m_{4i} m_{5i} R_{0i} + 8 m_{5i}^2) \times (m_{4i} R_{0i} \\ &\quad + m_{5i})^{3/2} \} + \frac{2 n_{1i} n_{10i}}{15 m_{4i}^3} \{ ((3 m_{2i} R_{1i} - 2 m_{5i})(m_{2i} R_{1i} + m_{5i})^{3/2} \\ &\quad - (3 m_{2i} R_{0i} - 2 m_{5i})(m_{2i} R_{0i} + m_{5i})^{3/2}) \} \end{aligned} \tag{8}$$

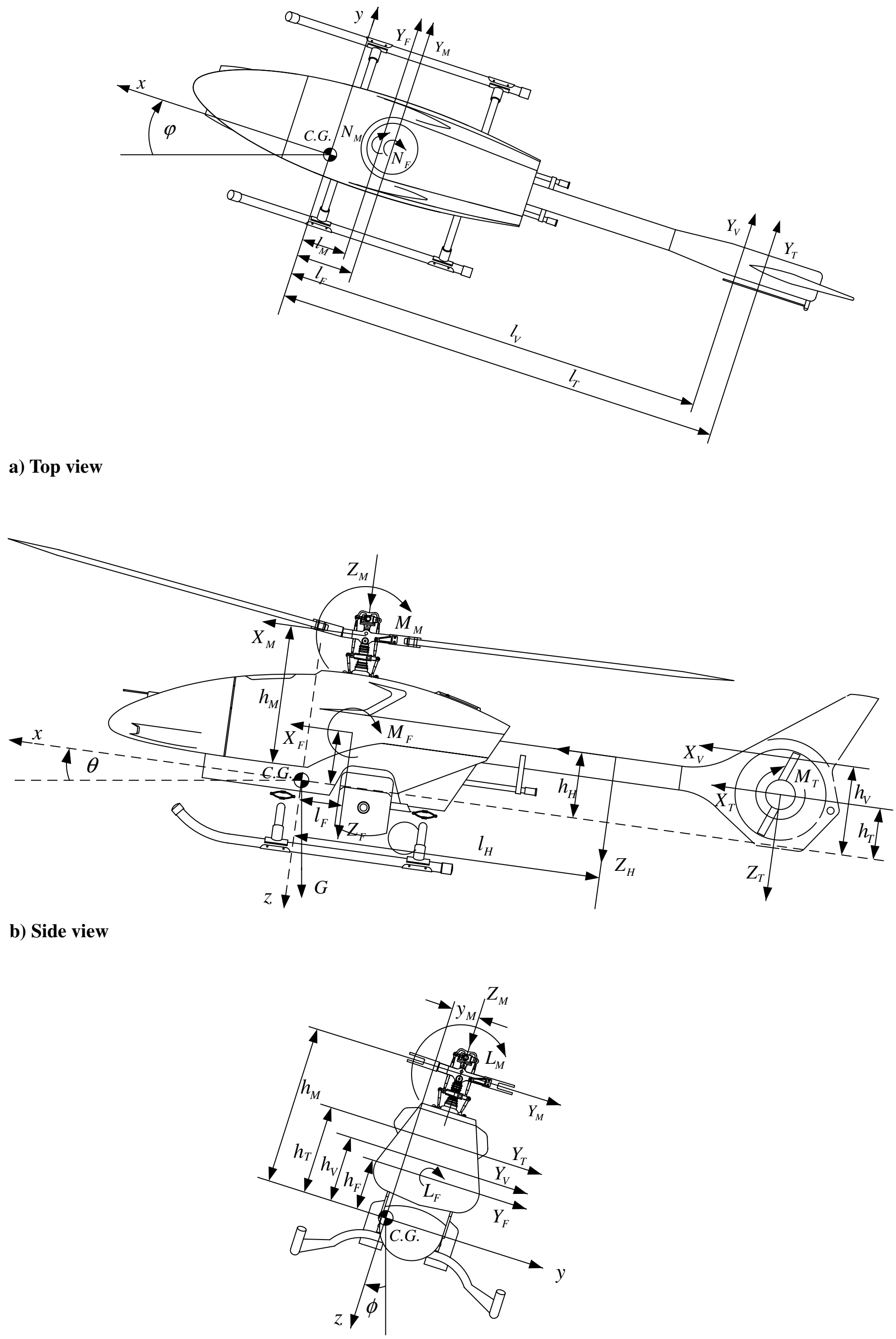

a) Top view

b) Side view

c) Back view

Fig. 2 Orthographic views of a helicopter.

where subscript i stands for M or T, for simplicity [4,18], and

$$m_{1i} = \frac{\Omega_i}{2} a_i b_i c_i + 4\pi V_c \qquad m_{2i} = 8\pi\Omega_i^2 a_i b_i c_i$$

$$m_{3i} = \frac{\rho}{2}\Omega_i a_i b_i c_i + 4\pi V_c \qquad m_{4i} = m_2\theta_{ci} \qquad m_{5i} = m_1^2 - \frac{V_c m_2}{\Omega_i}$$

$$m_{6i} = \frac{1}{\Omega_i}\left(\frac{m_1}{8\pi} - V_c\right) \tag{9}$$

$$n_{1i} = \frac{\rho}{2}\Omega_i^2 b_i c_i \qquad n_{2i} = V_c - \frac{m_{1i}}{8\pi} \qquad n_{3i} = \frac{a_i}{(8\pi\Omega_i)^2}$$

$$n_{4i} = m_{1i}^2 + m_{5i} \qquad n_{5i} = \frac{aV_c}{4\pi\Omega_i^2} \qquad n_{6i} = a_i\left(\frac{V_c}{\Omega_i}\right)^2$$

$$n_{7i} = \frac{a_i\theta_{ci}}{\Omega_i} n_{2i} - n_{3i} m_{4i} \qquad n_{8i} = \frac{a_i\theta_{ci}}{8\pi\Omega_i}$$

$$n_{9i} = n_{3i} n_{4i} - n_{5i} m_{1i} + n_{6i} \qquad n_{10i} = 2m_{1i} n_{3i} - n_{5i} \tag{10}$$

III. Simplified Helicopter Dynamics and Feedback Linearization

Even though it has been simplified, the dynamic model of the helicopter [Eqs. (4–10)] is still too complicated to be directly used in the design of the controller. In the following, the model is further simplified such that it can be feedback-linearized and a tracking controller can be then designed.

Under the condition of low velocity, we have

$$0 < \max(|a_{1s}|, |b_{1s}|, |T_T/T_M|) \ll 1 \tag{11}$$

The couplings term between rolling (pitching) moments and lateral (longitudinal) acceleration is relatively small and can be taken as uncertainty terms [18]. Thus, based on Eqs. (4–6), we have

$$\begin{aligned}\ddot{\boldsymbol{p}} = [0 \quad 0 \quad g]^T - \frac{1}{m}R[0 \quad 0 \quad T_M]^T + \bar{\boldsymbol{\Delta}}_F + \boldsymbol{\delta}_F \qquad \dot{R} = R\hat{\omega}\\ \dot{\boldsymbol{\omega}} = I_b^{-1}(\boldsymbol{M}_{\mathrm{ext}} - \boldsymbol{\omega} \times I_b\boldsymbol{\omega}) + \bar{\boldsymbol{\Delta}}_M\end{aligned} \tag{12}$$

where $\boldsymbol{\delta}_F$ is taken as the new uncertainty terms, expressed as

$$\boldsymbol{\delta}_F = \frac{1}{m}R\begin{bmatrix} -T_M \sin a_{1s} \\ T_M \sin b_{1s} - T_T \\ -T_M(\cos a_{1s}\cos b_{1s} - 1)\end{bmatrix} \tag{13}$$

Taking x, y, z, and ψ as outputs and $\ddot{T}_M$ and $\boldsymbol{M}_{\mathrm{ext}}$ as inputs and ignoring the terms of $\bar{\boldsymbol{\Delta}}_F + \boldsymbol{\delta}_F$ and $\bar{\boldsymbol{\Delta}}_M$, we have

$$\begin{aligned}\boldsymbol{p}^{(4)} &= -\frac{1}{m}R\{\boldsymbol{\omega} \times \{\boldsymbol{\omega} \times [0 \quad 0 \quad T_M]^T\}\}\\ &+ \frac{1}{m}R\begin{bmatrix} 0 & -T_M & 0 \\ T_M & 0 & 0 \\ 0 & 0 & 0\end{bmatrix} I_b^{-1}(\boldsymbol{M}_{\mathrm{ext}} - \boldsymbol{\omega} \times I_b\boldsymbol{\omega})\\ &- \frac{2}{m}R\{\boldsymbol{\omega} \times [0 \quad 0 \quad \dot{T}_M]^T\} - \frac{1}{m}R[0 \quad 0 \quad 1]^T\ddot{T}_M\end{aligned} \tag{14}$$

According to [4], the second equation of Eq. (12) is equivalent to the following:

$$\begin{bmatrix}\dot{\phi} \\ \dot{\theta} \\ \dot{\psi}\end{bmatrix} = \begin{bmatrix} 1 & \sin\phi\tan\theta & \cos\phi\tan\theta \\ 0 & \cos\phi & -\sin\phi \\ 0 & \sin\phi\sec\theta & \cos\phi\sec\theta\end{bmatrix}\begin{bmatrix} p \\ q \\ r\end{bmatrix} \tag{15}$$

It is not difficult to obtain

$$\begin{aligned}\ddot{\psi} &= -[0 \quad \sin\phi\sec\theta \quad \cos\phi\sec\theta]I_b^{-1}(\boldsymbol{\omega} \times I_b\boldsymbol{\omega})\\ &+ (q\cos\phi - r\sin\phi)\sec\theta[p + 2q\sin\phi\tan\theta + 2r\cos\phi\tan\theta]\\ &+ [0 \quad [0 \quad \sin\phi\sec\theta \quad \cos\phi\sec\theta]I_b^{-1}]\boldsymbol{M}_{\mathrm{ext}}\end{aligned} \tag{16}$$

From Eqs. (14) and (16), we have

$$\begin{aligned}\begin{bmatrix}\boldsymbol{p}^{(4)} \\ \ddot{\psi}\end{bmatrix} &= \begin{bmatrix} A_1(\phi, \theta, \psi, p, q, r, T_M, \dot{T}_M) \\ A_2(\phi, \theta, \psi, p, q, r)\end{bmatrix}\\ &+ \begin{bmatrix} B_1(\phi, \theta, \psi, T_M) \\ B_2(\phi, \theta, \psi)\end{bmatrix}\begin{bmatrix}\ddot{T}_M \\ \boldsymbol{M}_{\mathrm{ext}}\end{bmatrix} \qquad \boldsymbol{y} = [\boldsymbol{p}^T \quad \psi]^T\end{aligned} \tag{17}$$

where

$$\begin{aligned}A_1(\phi, \theta, \psi, p, q, r, T_M, \dot{T}_M) &= -\frac{1}{m}R\left[\boldsymbol{\omega} \times \left(\boldsymbol{\omega} \times \begin{bmatrix} 0 \\ 0 \\ T_M\end{bmatrix}\right)\right]\\ &- \frac{2}{m}R\left(\boldsymbol{\omega} \times \begin{bmatrix} 0 \\ 0 \\ \dot{T}_M\end{bmatrix}\right) + \frac{1}{m}R\left\{[I_b^{-1}(\boldsymbol{\omega} \times I_b\boldsymbol{\omega})] \times \begin{bmatrix} 0 \\ 0 \\ T_M\end{bmatrix}\right\}\end{aligned}$$

$$\begin{aligned}&B_1(\phi, \theta, \psi, T_M)\\ &= \left[\begin{matrix} -\frac{1}{m}R[0 \quad 0 \quad 1]^T & -\frac{T_M}{m}R\begin{bmatrix} 0 & 1 & 0 \\ -1 & 0 & 0 \\ 0 & 0 & 0\end{bmatrix}I_b^{-1}\end{matrix}\right]\\ &A_2(\phi, \theta, \psi, p, q, r) = -[0 \quad \sin\phi\sec\theta \quad \cos\phi\sec\theta]I_b^{-1}(\boldsymbol{\omega} \times I_b\boldsymbol{\omega})\\ &\quad + (q\cos\phi - r\sin\phi)\sec\theta[p + 2q\sin\phi\tan\theta + 2r\cos\phi\tan\theta]\\ &B_2(\phi, \theta, \psi) = [0 \quad [0 \quad \sin\phi\sec\theta \quad \cos\phi\sec\theta]I_b^{-1}]\end{aligned} \tag{18}$$

The following controller can be designed:

$$\begin{aligned}\begin{bmatrix}\ddot{T}_M \\ \boldsymbol{M}_{\mathrm{ext}}\end{bmatrix} &= \begin{bmatrix} B_1(\phi, \theta, \psi, T_M) \\ B_2(\phi, \theta, \psi)\end{bmatrix}^{-1}\left(\begin{bmatrix}\boldsymbol{p}_d^{(4)} + \boldsymbol{v}_1 \\ \ddot{\psi}_d + v_2\end{bmatrix}\right.\\ &\left. - \begin{bmatrix} A_1(\phi, \theta, \psi, p, q, r, T_M, \dot{T}_M) \\ A_2(\phi, \theta, \psi, p, q, r)\end{bmatrix}\right)\end{aligned} \tag{19}$$

where $\boldsymbol{v}_1$ and v_2 are two additional controls to be designed in Sec. IV.

By neglecting the disturbance and uncertainty terms, system (12) can be easily feedback-linearized by substituting Eq. (19) into Eq. (17). Therefore, we have the two linear systems below:

$$\boldsymbol{e}_1^{(4)} = \boldsymbol{v}_1 \tag{20}$$

and

$$\ddot{e}_2 = v_2 \tag{21}$$

where

$$\boldsymbol{e}_1 = \boldsymbol{p} - \boldsymbol{p}_d \qquad e_2 = \psi - \psi_d$$

are the tracking errors of positions and yaw angle, respectively.

Considering the disturbance and uncertainty terms in Eq. (12), we have

$$\begin{aligned}\ddot{\boldsymbol{e}}_1 = \boldsymbol{e}_3 + \bar{\boldsymbol{\Delta}}_F + \boldsymbol{\delta}_F \qquad \dot{\boldsymbol{e}}_3 = \boldsymbol{e}_4 \qquad \dot{\boldsymbol{e}}_4 = \boldsymbol{v}_1 + \tilde{\boldsymbol{\Delta}}_2\\ \ddot{e}_2 = v_2 + \tilde{\Delta}_3\end{aligned} \tag{22}$$

where

$$\begin{aligned}\boldsymbol{e}_3 &= [0 \quad 0 \quad g]^T - \frac{1}{m}R[0 \quad 0 \quad T_M]^T - \ddot{\boldsymbol{p}}_d\\ \boldsymbol{e}_4 = \dot{\boldsymbol{e}}_3 &= -\frac{1}{m}R(\boldsymbol{\omega} \times [0 \quad 0 \quad T_M]^T) - \frac{1}{m}R[0 \quad 0 \quad \dot{T}_M]^T - \dddot{\boldsymbol{p}}_d\\ \tilde{\boldsymbol{\Delta}}_2 &= -\frac{T_M}{m}R\begin{bmatrix} 0 & 1 & 0 \\ -1 & 0 & 0 \\ 0 & 0 & 0\end{bmatrix}\bar{\boldsymbol{\Delta}}_M\\ \tilde{\Delta}_3 &= [0 \quad \sin\phi\sec\theta \quad \cos\phi\sec\theta]\bar{\boldsymbol{\Delta}}_M\end{aligned} \tag{23}$$

Unlike $\bar{\boldsymbol{\Delta}}_F$, $\tilde{\boldsymbol{\Delta}}_2$, and $\tilde{\Delta}_3$, the uncertainty term $\boldsymbol{\delta}_F$ in Eq. (22), which is closely related to the state, is not mixed up with any other external disturbances and can be regarded as uncertainty with some unknown or omitted parameters. To do so, we first make some changes to Eq. (22).

Let

$$\Upsilon = -\begin{bmatrix} 1 & 0 & -\sin a_{1s} \\ 0 & 1 & \sin b_{1s} - \frac{T_T}{T_M} \\ 0 & 0 & 1 - \cos a_{1s}\cos b_{1s} \end{bmatrix} \tag{24}$$

Suppose the 2-norm of matrix is selected with the conditions 1) $-30^\circ < a_{1s} < 30^\circ, -30^\circ < b_{1s} < 30^\circ$ (input constraints in Sec. V) and 2) $T_T/T_M \le 0.225$ (for the helicopter model used in Sec. V). Thus, for any real vector $[\,a \quad b \quad c\,]^T$, we have

$$\begin{aligned}\|\Upsilon\| &= \frac{\max \left\|\Upsilon\begin{bmatrix} a \\ b \\ c\end{bmatrix}\right\|_2}{\sqrt{a^2+b^2+c^2}} = \sqrt{\frac{(a - c\sin a_{1s})^2 + [b + c(\sin b_{1s} - \frac{T_T}{T_M})]^2 + c^2(1-\cos a_{1s}\cos b_{1s})^2}{a^2+b^2+c^2}} \\ &= \sqrt{\frac{a^2+b^2+c^2[\sin^2 a_{1s} + (\sin b_{1s} - \frac{T_T}{T_M})^2 + (1-\cos a_{1s}\cos b_{1s})^2] - 2ac\sin a_{1s} + 2bc(\sin b_{1s} - \frac{T_T}{T_M})}{a^2+b^2+c^2}} \\ &\le \sqrt{\frac{a^2+b^2+c^2[0.25 + (0.25+0.225)^2 + 1] + 0.5a^2 + 0.5c^2 + (b^2+c^2)(0.5+0.225)}{a^2+b^2+c^2}} \\ &\le \sqrt{1.725 + \frac{c^2[0.25 + (0.25+0.225)^2] + 0.5c^2}{a^2+b^2+c^2}} < \sqrt{3}\end{aligned} \tag{25}$$

With Eq. (25), the following equation can be obtained:

$$\begin{aligned}&\| -R\Upsilon R^{-1}[0 \quad 0 \quad g]^T + \boldsymbol{\delta}_F - R\Upsilon R^{-1}\ddot{\boldsymbol{p}}_{\boldsymbol{d}}\| \\ &= \left\|\frac{1}{m}R\begin{bmatrix} -T_M\sin a_{1s} \\ T_M\sin b_{1s} - T_T \\ -T_M(\cos a_{1s}\cos b_{1s} - 1)\end{bmatrix} - R\Upsilon R^{-1}\begin{bmatrix}0\\0\\g\end{bmatrix}\right. \\ &\left. - R\Upsilon R^{-1}\ddot{\boldsymbol{p}}_{\boldsymbol{d}}\right\| = \left\| R\Upsilon\left\{\frac{1}{m}\Upsilon^{-1}\begin{bmatrix} -T_M\sin a_{1s} \\ T_M\sin b_{1s} - T_T \\ -T_M(\cos a_{1s}\cos b_{1s} - 1)\end{bmatrix}\right.\right. \\ &\left.\left. - R^{-1}\begin{bmatrix}0\\0\\g\end{bmatrix} - R^{-1}\ddot{\boldsymbol{p}}_{\boldsymbol{d}}\right\}\right\| = \left\| R\Upsilon R^{-1}\left\{\frac{1}{m}R[0 \quad 0 \quad T_M]^T\right.\right. \\ &\left.\left. - \begin{bmatrix}0\\0\\g\end{bmatrix} - \ddot{\boldsymbol{p}}_{\boldsymbol{d}}\right\}\right\| \le \|R\Upsilon R^{-1}\|\|\boldsymbol{e}_3\| \le \sqrt{3}\|\boldsymbol{e}_3\|\end{aligned} \tag{26}$$

Then Eq. (22) can be rewritten as

$$\ddot{\boldsymbol{e}}_1 = \boldsymbol{e}_3 + \tilde{\boldsymbol{\Delta}}_1 + \tilde{\boldsymbol{\delta}}_1 \qquad \dot{\boldsymbol{e}}_3 = \boldsymbol{e}_4 \qquad \dot{\boldsymbol{e}}_4 = \boldsymbol{v}_1 + \tilde{\boldsymbol{\Delta}}_2$$
$$\ddot{e}_2 = v_2 + \tilde{\Delta}_3 \tag{27}$$

where

$$\begin{aligned}\tilde{\boldsymbol{\delta}}_1 &= -R\Upsilon R^{-1}[0 \quad 0 \quad g]^T + \boldsymbol{\delta}_F - R\Upsilon R^{-1}\ddot{\boldsymbol{p}}_{\boldsymbol{d}} \\ \tilde{\boldsymbol{\Delta}}_1 &= \bar{\boldsymbol{\Delta}}_F + R\Upsilon R^{-1}[0 \quad 0 \quad g]^T + R\Upsilon R^{-1}\ddot{\boldsymbol{p}}_{\boldsymbol{d}}\end{aligned} \tag{28}$$

and $\tilde{\boldsymbol{\delta}}_1$ satisfies inequality

$$\|\tilde{\boldsymbol{\delta}}_1\| \le \sqrt{3}\|\boldsymbol{e}_3\| \tag{29}$$

The new disturbance term $\tilde{\boldsymbol{\Delta}}_1$ includes the original disturbance $\bar{\boldsymbol{\Delta}}_F$ and other two new terms, and hence the state variables have little influence on $\tilde{\boldsymbol{\Delta}}_1$, because the only term related to state variables is R, which satisfies $\|R\|_2 = 1$. In the end, we obtain a model (27) with external disturbances and bounded uncertainties.

So far we have not considered the aerodynamics effect. The aerodynamics here is a static relation, as expressed by Eqs. (6–10), between the real input (two collective pitches and two cyclic pitches) and the forces/moments. According to [18], they can be simplified as

$$\begin{aligned}L^s = S_{L1}b_{1s} + S_{L2}Q_M^s, \qquad M^s &= S_{M1}a_{1s} + S_{M2}T_M^s + S_{M3}Q_T^s \\ N^s = S_{N1}Q_M^s + S_{N2}T_T^s, \qquad T_M^s &= S_{T_M1}\theta_M + S_{T_M2} \\ T_T^s = S_{T_T1}\theta_T + S_{T_T2}, \qquad Q_M^s &= S_{Q_M1}\theta_M + S_{Q_M2} \\ Q_T^s &= S_{Q_T1}\theta_T + S_{Q_T2}\end{aligned} \tag{30}$$

where S_* are some known constants. Therefore, the helicopter control inputs a_{1s}, b_{1s}, θ_M, and θ_T can be expressed using T_M^s, L^s, M^s, and N^s:

$$\begin{bmatrix} a_{1s} \\ b_{1s} \\ \theta_M \\ \theta_T\end{bmatrix} = \begin{bmatrix} 0 & S_{L1} & S_{L2}S_{Q_M1} & 0 \\ S_{M1} & 0 & S_{M2}S_{T_M1} & S_{M3}S_{Q_T} \\ 0 & 0 & S_{N1}S_{Q_M1} & S_{N2}S_{T_T} \\ 0 & 0 & S_{T_M1} & 0\end{bmatrix}^{-1}\left(\begin{bmatrix} L^s \\ M^s \\ N^s \\ T_M^s\end{bmatrix} - \begin{bmatrix} S_{L2}S_{Q_M2} \\ S_{M3}S_{Q_T2} + S_{M2}S_{T_M2} \\ S_{N2}S_{T_T2} + S_{N1}S_{Q_M2} \\ S_{T_M2}\end{bmatrix}\right) \tag{31}$$

Based on Eqs. (12) and (22), we rewrite the feedback linearization model (27) as

$$\ddot{\boldsymbol{e}}_1 = \boldsymbol{e}_3 + \boldsymbol{\Delta}_1 + \boldsymbol{\delta}_1 \qquad \dot{\boldsymbol{e}}_3 = \boldsymbol{e}_4 \qquad \dot{\boldsymbol{e}}_4 = \boldsymbol{v}_1 + \boldsymbol{\Delta}_2 \tag{32}$$

and

$$\ddot{e}_2 = v_2 + \Delta_3 \tag{33}$$

where

$$
\begin{gathered}
\boldsymbol{\delta}_1 = \tilde{\boldsymbol{\delta}}_1 \qquad \boldsymbol{\Delta}_1 = \tilde{\boldsymbol{\Delta}}_1 + \frac{1}{m} R(\psi, \phi, \theta) \boldsymbol{\delta}_2 \\
\boldsymbol{\Delta}_2 = \frac{T_M}{m} R(\psi, \phi, \theta) \begin{bmatrix} 0 & 1 & 0 \\ -1 & 0 & 0 \\ 0 & 0 & 0 \end{bmatrix} I_b^{-1} (I_b \bar{\boldsymbol{\Delta}}_M + \boldsymbol{\delta}_3) \\
\Delta_3 = [0 \quad \sin\phi \sec\theta \quad \cos\phi \sec\theta] I_b^{-1} (I_b \bar{\boldsymbol{\Delta}}_M + \boldsymbol{\delta}_3) \\
\boldsymbol{\delta}_2 = [0 \quad 0 \quad -T_M]^T - [0 \quad 0 \quad -T_M^s]^T \qquad \boldsymbol{\delta}_3 = \boldsymbol{M}_{\text{ext}} - \boldsymbol{M}_s
\end{gathered} \tag{34}
$$

in which $\boldsymbol{\delta}_2$ and $\boldsymbol{\delta}_3$ are the uncertainty terms due to the inaccurate or simplified aerodynamics from Eqs. (7–10) and (30). They can be regarded as the disturbances, since they are not related to the state variables ($\boldsymbol{e}_1$, $\boldsymbol{e}_2$, $\boldsymbol{e}_3$, and $\boldsymbol{e}_4$) of the simplified helicopter model.

IV. Acceleration-Feedback-Enhanced Robust Control

A. Nonlinear H_∞ Control Without Disturbance Information

From the preceding analysis, we can transform the helicopter model into two different linear models with external disturbances and nonlinear inner uncertainties as Eqs. (32) and (33) by using the feedback linearization technique. In fact, Eqs. (32) and (33) can be denoted as

$$
\dot{\boldsymbol{x}} = A\boldsymbol{x} + B\boldsymbol{v} + f(\boldsymbol{x}) + D\boldsymbol{\Delta} \qquad \boldsymbol{y} = C\boldsymbol{x} \tag{35}
$$

where $\boldsymbol{x}$ is the state vector; $\boldsymbol{v}$ is the input vector; $\boldsymbol{\Delta}$ is the external disturbances; $\boldsymbol{y}$ is the output vector; A, B, C, and D are all constant matrices with proper dimension; $f(\boldsymbol{x})$ is the nonlinear uncertainty term; and

$$
\begin{gathered}
\boldsymbol{x} = [\,(\boldsymbol{x}_1^T) \quad (\boldsymbol{x}_2^T)_{1\times\bar{n}} \quad (\boldsymbol{x}_3^T)_{1\times\bar{n}} \quad \cdots \quad (\boldsymbol{x}_n^T)_{1\times\bar{n}}\,]_{n\times 1}^T \\
A = \begin{bmatrix} 0_{\bar{n}\times\bar{n}} & I_{\bar{n}} & 0_{\bar{n}\times\bar{n}} & \cdots & 0_{\bar{n}\times\bar{n}} \\ 0_{\bar{n}\times\bar{n}} & 0_{\bar{n}\times\bar{n}} & I_{\bar{n}} & \cdots & 0_{\bar{n}\times\bar{n}} \\ 0_{\bar{n}\times\bar{n}} & 0_{\bar{n}\times\bar{n}} & 0_{\bar{n}\times\bar{n}} & \cdots & 0_{\bar{n}\times\bar{n}} \\ \vdots & \vdots & \vdots & \ddots & \vdots \\ 0_{\bar{n}\times\bar{n}} & 0_{\bar{n}\times\bar{n}} & 0_{\bar{n}\times\bar{n}} & \cdots & 0_{\bar{n}\times\bar{n}} \end{bmatrix}_{n\times n}, \qquad B = \begin{bmatrix} 0_{\bar{n}\times\bar{m}} \\ 0_{\bar{n}\times\bar{n}} \\ 0_{\bar{n}\times\bar{n}} \\ \vdots \\ I_{\bar{n}} \end{bmatrix} \\
D = [(\boldsymbol{d}_{i,j})_{\bar{n}\times 1}]_{n\times\bar{m}}, \qquad C = [\,I_{\bar{n}} \quad 0_{\bar{n}\times\bar{n}} \quad 0_{\bar{n}\times\bar{n}} \quad \cdots \quad 0_{\bar{n}\times\bar{n}}\,]_{1\times n}
\end{gathered} \tag{36}
$$

Furthermore, $f(\boldsymbol{x})$ satisfies the condition

$$
\|f(\boldsymbol{x})\| \le \sigma \|\boldsymbol{x}\| \tag{37}
$$

For system (32), we have

$$
\begin{gathered}
\bar{n} = 3 \qquad \bar{m} = 6 \qquad \boldsymbol{x}_1 = \boldsymbol{e}_1 \qquad \boldsymbol{x}_2 = \dot{\boldsymbol{e}}_1 \qquad \boldsymbol{x}_3 = \boldsymbol{e}_3 \\
\boldsymbol{x}_4 = \boldsymbol{e}_4 \qquad \boldsymbol{v} = \boldsymbol{v}_1 \qquad \boldsymbol{x} = [\boldsymbol{x}_1^T \quad \boldsymbol{x}_2^T \quad \boldsymbol{x}_3^T \quad \boldsymbol{x}_4^T]^T \\
\boldsymbol{\Delta} = [\,\boldsymbol{\Delta}_1^T \quad \boldsymbol{\Delta}_2^T\,]^T \qquad A = \begin{bmatrix} 0_{3\times 3} & I_3 & 0_{3\times 3} & 0_{3\times 3} \\ 0_{3\times 3} & 0_{3\times 3} & I_3 & 0_{3\times 3} \\ 0_{3\times 3} & 0_{3\times 3} & 0_{3\times 3} & I_3 \\ 0_{3\times 3} & 0_{3\times 3} & 0_{3\times 3} & 0_{3\times 3} \end{bmatrix} \\
B = \begin{bmatrix} 0_{3\times 3} \\ 0_{3\times 3} \\ 0_{3\times 3} \\ I_{3\times 3} \end{bmatrix} \qquad C = [\,I_{3\times 3} \quad 0_{3\times 3} \quad 0_{3\times 3} \quad 0_{3\times 3}\,] \\
D = \begin{bmatrix} 0_{3\times 3} & 0_{3\times 3} \\ I_{3\times 3} & 0_{3\times 3} \\ 0_{3\times 3} & 0_{3\times 3} \\ 0_{3\times 3} & I_{3\times 3} \end{bmatrix}
\end{gathered} \tag{38}
$$

Based on Eqs. (29) and (34), we have

$$
\sigma = \sqrt{3} \tag{39}
$$

Similarly, system (33) can also be written in the form of Eqs. (35) with

$$
\begin{gathered}
\bar{n} = 1 \qquad \bar{m} = 1 \qquad \boldsymbol{x}_1 = e_2 \qquad \boldsymbol{x}_2 = \dot{e}_2 \qquad \boldsymbol{v} = v_2 \\
x = [x_1 \quad x_2]^T \qquad \Delta = \Delta_3 \qquad A = \begin{bmatrix} 0 & 1 \\ 0 & 0 \end{bmatrix} \qquad B = \begin{bmatrix} 0 \\ 1 \end{bmatrix} \\
C = [1 \quad 0] \qquad D = \begin{bmatrix} 0 \\ 1 \end{bmatrix}
\end{gathered} \tag{40}
$$

and

$$
\sigma = 0 \tag{41}
$$

In the rest of this subsection, we will design an H_∞ robust controller dealing with both the external disturbance Δ and the nonlinear uncertainties term $f(\boldsymbol{x})$ to ensure the closed-loop stability and the robust performance of the closed-loop system. The main result is stated in the following theorem.

Theorem I: If a linear feedback controller $\boldsymbol{v} = K\boldsymbol{x}$ and a positive definite matrix P can be found satisfying the following inequality,

$$
P(A + BK) + (A^T + K^T B^T)P + (1 + \sigma^2)P + \frac{2}{\gamma^2} PDD^T P + \frac{1}{2} C^T C \le 0 \tag{42}
$$

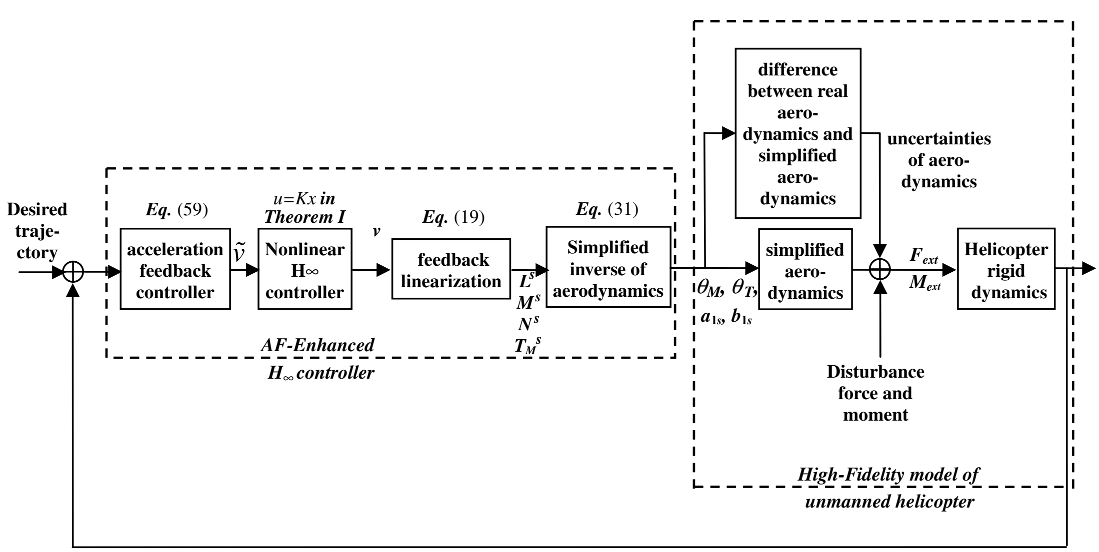

Fig. 3 Controller structure.

Table 1 Parameters for helicopter simulation

Parameter	Description
$m = 9.5$ kg	Helicopter mass
$\rho = 1.2$ kg/m^3	Air density
$I_{xx} = 0.1634$ kgm^2	Inertia on X axis
$I_{yy} = 0.5782$ kgm^2	Inertia on Y axis
$I_{zz} = 0.6306$ kgm^2	Inertia on Z axis
$h_M = 0.2340$ m	Distance to c.g.
$y_M = 0$ m	Distance to c.g.
$l_M = 0.01$ m	Distance to c.g.
$h_T = 0.062$ m	Distance to c.g.
$L_T = 0.898$ m	Distance to c.g.
$\Omega_M = 171.1$ rad/s	Angular velocity of main rotor
$a_M = 5.4$ rad^{-1}	Slope of lift curve of main rotor
$b_M = 2$	Number of main blade
$c_M = 0.058$ m	Width of main rotor
$R_M = 0.79$ m	Radius of main rotor
$R_{0M} = 0.196$ m	Inner radius of main rotor
$\Omega_T = 920.8$ rad/s	Angular velocity of tail rotor
$a_T = 5.4$ rad^{-1}	Slope of lift curve of tail rotor
$b_T = 2$	Number of tail blade
$c_T = 0.028$ m	Width of tail rotor
$R_T = 0.1290$ m	Radius of tail rotor
$R_{0T} = 0.042$ m	Inner radius of tail rotor

then system (35) is finite-gain L_2-stable from disturbances $\boldsymbol{\Delta}$ to outputs $\boldsymbol{y}$ for all the allowable $f(.)$, and the L_2 gain is less than or equal to γ.

Proof: First, let

$$V(\boldsymbol{x}) = \boldsymbol{x}^T P \boldsymbol{x} \tag{43}$$

be the Lyapunov function candidate of system (35), where P is a positive definite matrix with proper dimensions.

Computing the derivative of $V(\boldsymbol{x})$ along the trajectory of the system (35), we have

$$\begin{aligned}\dot{V}(\boldsymbol{x}) &= V_x[A\boldsymbol{x} + BK\boldsymbol{x} + f(\boldsymbol{x})] + V_x D\boldsymbol{\Delta} = 2\boldsymbol{x}^T P[A\boldsymbol{x} + BK\boldsymbol{x} \\ &\quad + f(\boldsymbol{x})] + 2\boldsymbol{x}^T PD\boldsymbol{\Delta} = -\frac{\gamma^2}{2}\left\|\boldsymbol{\Delta} - \frac{2}{\gamma^2}D^T P\boldsymbol{x}\right\|_2^2 + 2\boldsymbol{x}^T P[A\boldsymbol{x} \\ &\quad + BK\boldsymbol{x} + f(\boldsymbol{x})] + \frac{2}{\gamma^2}\boldsymbol{x}^T PDD^T P\boldsymbol{x} + \frac{\gamma^2}{2}\|\boldsymbol{\Delta}\|_2^2\end{aligned} \tag{44}$$

If the following inequality is satisfied for all allowable state x,

$$\begin{aligned}&\boldsymbol{x}^T P[A\boldsymbol{x} + BK\boldsymbol{x} + f(\boldsymbol{x})] + [\boldsymbol{x}^T A^T + \boldsymbol{x}^T K^T B^T + f^T(\boldsymbol{x})]P\boldsymbol{x} \\ &\quad + \frac{2}{\gamma^2}\boldsymbol{x}^T PDD^T P\boldsymbol{x} + \frac{1}{2}\boldsymbol{x}^T C^T C\boldsymbol{x} \le 0\end{aligned} \tag{45}$$

We have

$$\begin{bmatrix} (A + (1+\sigma^2)I/2)X + BW + [(A + (1+\sigma^2)I/2)X + BW]^T & D & \gamma^{-1}(CX)^T \\ D^T & -I & 0 \\ \gamma^{-1}CX & 0 & -I \end{bmatrix} \le 0 \qquad \boldsymbol{v} = WX^{-1}\boldsymbol{x} \tag{55}$$

$$\dot{V}(\boldsymbol{x}) \le \frac{\gamma^2}{2}\|\boldsymbol{\Delta}\|_2^2 - \frac{1}{2}\|\boldsymbol{y}\|_2^2 - \frac{\gamma^2}{2}\left\|\boldsymbol{\Delta} - \frac{1}{\gamma^2}D^T P\boldsymbol{x}\right\|_2^2 \tag{46}$$

and

$$\dot{V}(\boldsymbol{x}) \le \tfrac{1}{2}\gamma^2\|\boldsymbol{\Delta}\|_2^2 - \tfrac{1}{2}\|\boldsymbol{y}\|_2^2 \tag{47}$$

Integrating Eq. (47) yields

$$V(\boldsymbol{x}(\tau)) - V(\boldsymbol{x}_0) \le \frac{1}{2}\gamma^2\int_0^\tau \|\boldsymbol{\Delta}\|_2^2\,\mathrm{d}t - \frac{1}{2}\int_0^\tau \|\boldsymbol{y}\|_2^2\,\mathrm{d}t \tag{48}$$

From $V(\boldsymbol{x}) \ge 0$, we obtain

$$\begin{aligned}\int_0^\tau \|\boldsymbol{y}\|_2^2\,\mathrm{d}t &\le \gamma^2\int_0^\tau \|\boldsymbol{\Delta}\|_2^2\,\mathrm{d}t - 2V(\boldsymbol{x}(\tau)) + 2V(\boldsymbol{x}_0) \\ &\le \gamma^2\int_0^\tau \|\boldsymbol{\Delta}\|_2^2\,\mathrm{d}t + 2V(\boldsymbol{x}_0)\end{aligned} \tag{49}$$

Computing the square roots and using the inequality $\sqrt{a^2+b^2} \le a + b$ for nonnegative numbers a and b, we obtain

$$\|\boldsymbol{y}\|_{L_2} \le \gamma\|\boldsymbol{\Delta}\|_{L_2} + \sqrt{2V(\boldsymbol{x}_0)} \tag{50}$$

Thus, we can conclude that if the inequality (45) is satisfied for all allowable $\boldsymbol{x}$, system (35) can be guaranteed to be finite-gain L_2-stable from $\boldsymbol{\Delta}$ to $\boldsymbol{y}$, and the L_2 gain is less than or equal to γ.

Since $\|f(\boldsymbol{x})\| \le \sigma\|\boldsymbol{x}\|$, we have

$$\begin{aligned}&\boldsymbol{x}^T Pf(\boldsymbol{x}) + f^T(\boldsymbol{x})P\boldsymbol{x} = -[\boldsymbol{x}^T - f^T(\boldsymbol{x})]P[\boldsymbol{x} - f(\boldsymbol{x})] + \boldsymbol{x}^T P\boldsymbol{x} \\ &\quad + f^T(\boldsymbol{x})Pf(\boldsymbol{x}) \le \boldsymbol{x}^T P\boldsymbol{x} + f^T(\boldsymbol{x})Pf(\boldsymbol{x}) \le (1+\sigma^2)\boldsymbol{x}^T P\boldsymbol{x}\end{aligned} \tag{51}$$

Thus,

$$\begin{aligned}&\boldsymbol{x}^T P[A\boldsymbol{x} + BK\boldsymbol{x} + f(\boldsymbol{x})] + [\boldsymbol{x}^T A^T + \boldsymbol{x}^T K^T B^T + f^T(\boldsymbol{x})]P\boldsymbol{x} \\ &\quad + \frac{2}{\gamma^2}\boldsymbol{x}^T PDD^T P\boldsymbol{x} + \frac{1}{2}\boldsymbol{x}^T C^T C\boldsymbol{x} \\ &\le \boldsymbol{x}^T P(A + BK)\boldsymbol{x} + \boldsymbol{x}^T(A^T + K^T B^T)P\boldsymbol{x} + (1+\sigma^2)\boldsymbol{x}^T P\boldsymbol{x} \\ &\quad + \frac{2}{\gamma^2}\boldsymbol{x}^T PDD^T P\boldsymbol{x} + \frac{1}{2}\boldsymbol{x}^T C^T C\boldsymbol{x}\end{aligned} \tag{52}$$

This means that if we can select a feedback $\boldsymbol{u} = K\boldsymbol{x}$ such that Eq. (42) is negative definite, then inequality (45) can be satisfied for all allowable $\boldsymbol{x}$. Furthermore, the system (35) is finite-gain L_2-stable from disturbances $\boldsymbol{\Delta}$ to outputs $\boldsymbol{y}$, and the L_2 gain is less than or equal to γ. □

Equation (42) can be rewritten as

$$\begin{aligned}&P\left(A + BK + \frac{1+\sigma^2}{2}I\right) + \left(A^T + K^T B^T + \frac{1+\sigma^2}{2}I\right)P \\ &\quad + \frac{2}{\gamma^2}PDD^T P + \frac{1}{2}C^T C \le 0\end{aligned} \tag{53}$$

It is well known in linear H_∞ theory that the problem is equivalent to finding a state feedback $\boldsymbol{u} = K\boldsymbol{x}$ such that the following system has H_∞-norm less than or equal to γ from disturbances to outputs:

$$\dot{\boldsymbol{x}} = \left(A + \frac{1+\sigma^2}{2}I\right)\boldsymbol{x} + B\boldsymbol{v} + D\boldsymbol{\Delta} \qquad \boldsymbol{y} = C\boldsymbol{x} \tag{54}$$

This can be easily solved using linear robust control theory. According to [19], the preceding problem is equivalent to solving the following linear matrix inequalities (LMIs) (W and X are unknown matrices to be computed):

B. Robust Control with Acceleration Feedback

In the last section, the H_∞ controller was designed with respect to system (35). However, the H_∞ control is conservative as it supposes that the uncertainties are all unknown, which limits the performance of the closed-loop system. In the following, an acceleration-feedback-enhanced H_∞ robust control method is designed.

First, Eq. (35) is rewritten by taking $f(\boldsymbol{x})$ as a new disturbance signal with $\boldsymbol{v} = K\boldsymbol{x} + \tilde{\boldsymbol{v}}$ designed:

$$\dot{\boldsymbol{x}} = (A + BK)\boldsymbol{x} + B\tilde{\boldsymbol{v}} + D\hat{\boldsymbol{\Delta}} \tag{56}$$

where K is the linear H_∞ feedback control gain designed in Sec. IV.A.

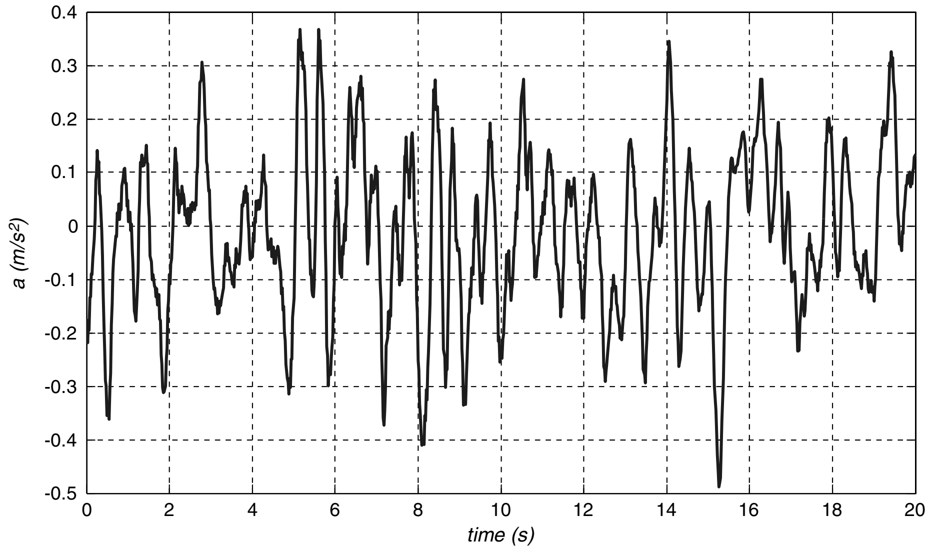

Fig. 4 Measured linear acceleration flight-test data.

In system (56), the uncertainty term $f(\boldsymbol{x})$ has been taken as parts of the disturbances of $\boldsymbol{\Delta}$, and $\hat{\boldsymbol{\Delta}}$ is the newly defined disturbance terms.

To present our main idea about how to attenuate disturbances, we first introduce some new variables $\xi_1, \xi_2, \ldots, \xi_m$ and let

$$\hat{\boldsymbol{x}} = \begin{bmatrix} \boldsymbol{x}_1 \\ \boldsymbol{x}_2 - \boldsymbol{d}_{1,1}\xi_1 - \cdots - \boldsymbol{d}_{1,m}\xi_m \\ \boldsymbol{x}_3 - \boldsymbol{d}_{1,1}\dot{\xi}_1 - \cdots - \boldsymbol{d}_{1,m}\dot{\xi}_m - \boldsymbol{d}_{2,1}\xi_1 - \cdots - \boldsymbol{d}_{2,m}\xi_m \\ \vdots \\ \boldsymbol{x}_n - \boldsymbol{d}_{1,1}\xi_1^{(n-2)} - \cdots - \boldsymbol{d}_{1,m}\xi_m^{(n-2)} - \cdots - \boldsymbol{d}_{n-1,1}\xi_1 - \cdots - \boldsymbol{d}_{n-1,m}\xi_m \end{bmatrix}_{n\times 1} \tag{57}$$

We have

$$\begin{aligned} \dot{\hat{\boldsymbol{x}}}_1 &= \dot{\boldsymbol{x}}_1 = \boldsymbol{x}_{1,1} + \boldsymbol{d}_{1,1}\Delta_1 + \cdots + \boldsymbol{d}_{1,m}\Delta_m = \hat{\boldsymbol{x}}_2 + \boldsymbol{d}_{1,1}(\Delta_1 + \xi_1) \\ &\quad + \cdots + \boldsymbol{d}_{1,m}(\Delta_m + \xi_m) \\ \dot{\hat{\boldsymbol{x}}}_2 &= \dot{\boldsymbol{x}}_2 - \boldsymbol{d}_{1,1}\dot{\xi}_1 - \cdots - \boldsymbol{d}_{1,m}\dot{\xi}_m = \boldsymbol{x}_3 - \boldsymbol{d}_{1,1}\dot{\xi}_1 - \cdots - \boldsymbol{d}_{1,m}\dot{\xi}_m \\ &\quad + \boldsymbol{d}_{2,1}\Delta_1 + \cdots + \boldsymbol{d}_{2,m}\Delta_m = \hat{\boldsymbol{x}}_4 + \boldsymbol{d}_{2,1}(\Delta_1 + \xi_1) + \cdots \\ &\quad + \boldsymbol{d}_{2,m}(\Delta_m + \xi_m) \cdots \dot{\hat{\boldsymbol{x}}}_n = \dot{\boldsymbol{x}}_n - \boldsymbol{d}_{1,1}\xi_1^{(n-1)} - \cdots - \boldsymbol{d}_{1,m}\xi_m^{(n-1)} \\ &\quad - \cdots - \boldsymbol{d}_{n-1,1}\dot{\xi}_1 - \cdots - \boldsymbol{d}_{n-1,m}\dot{\xi}_m = \tilde{\boldsymbol{v}} + \boldsymbol{k}_1\boldsymbol{x}_1 + \boldsymbol{k}_2\boldsymbol{x}_2 + \cdots \\ &\quad + \boldsymbol{k}_n\boldsymbol{x}_n - \boldsymbol{d}_{1,1}\xi_1^{(n-1)} - \cdots - \boldsymbol{d}_{1,m}\xi_m^{(n-1)} - \cdots - \boldsymbol{d}_{n-1,1}\dot{\xi}_1 - \cdots \\ &\quad - \boldsymbol{d}_{n-1,m}\dot{\xi}_m + \boldsymbol{d}_{n,1}\Delta_1 + \cdots + \boldsymbol{d}_{n,m}\Delta_m = \tilde{\boldsymbol{v}} + \boldsymbol{k}_1\hat{\boldsymbol{x}}_1 + \boldsymbol{k}_2\hat{\boldsymbol{x}}_2 \\ &\quad + \cdots + \boldsymbol{k}_n\hat{\boldsymbol{x}}_n + [\boldsymbol{k}_2(\boldsymbol{d}_{1,1}\xi_1 + \cdots + \boldsymbol{d}_{1,m}\xi_m) + \cdots \\ &\quad + \boldsymbol{k}_n(\boldsymbol{d}_{1,1}\xi_1^{(n-2)} + \cdots + \boldsymbol{d}_{1,m}\xi_m^{(n-2)} + \cdots + \boldsymbol{d}_{n-1,1}\xi_1 + \cdots \\ &\quad + \boldsymbol{d}_{n-1,m}\xi_m)] - \boldsymbol{d}_{1,1}\xi_1^{(n-1)} - \cdots - \boldsymbol{d}_{1,m}\xi_m^{(n-1)} - \cdots - \boldsymbol{d}_{n-1,1}\dot{\xi}_1 \\ &\quad - \cdots - \boldsymbol{d}_{n-1,m}\dot{\xi}_m - \boldsymbol{d}_{n,1}\xi_1 - \cdots - \boldsymbol{d}_{n,m}\xi_m + \boldsymbol{d}_{n,1}(\Delta_1 + \xi_1) \\ &\quad + \cdots + \boldsymbol{d}_{n,m}(\Delta_m + \xi_m) \end{aligned} \tag{58}$$

Subsequently, if the control input $\tilde{\boldsymbol{v}}$ is designed as

Table 2 Five simulations conducted in this paper

Experiment 1	Simulation without force and moment disturbances
Experiment 2	Simulation with only step force disturbances
Experiment 3	Simulation with only sine force disturbances
Experiment 4	Simulation with only step moment disturbances
Experiment 5	Simulation with only sine moment disturbances

$$\begin{aligned} \tilde{\boldsymbol{v}} &= \boldsymbol{d}_{1,1}\xi_1^{(n-1)} + \cdots + \boldsymbol{d}_{1,m}\xi_m^{(n-1)} + \cdots + \boldsymbol{d}_{n-1,1}\dot{\xi}_1 + \cdots \\ &\quad + \boldsymbol{d}_{n-1,m}\dot{\xi}_m + \boldsymbol{d}_{n,1}\xi_1 + \cdots + \boldsymbol{d}_{n,m}\xi_m - [\boldsymbol{k}_2(\boldsymbol{d}_{1,1}\xi_1 + \cdots \\ &\quad + \boldsymbol{d}_{1,m}\xi_m) + \cdots + \boldsymbol{k}_n(\boldsymbol{d}_{1,1}\xi_1^{(n-2)} + \cdots + \boldsymbol{d}_{1,m}\xi_m^{(n-2)} + \cdots \\ &\quad + \boldsymbol{d}_{n-1,1}\xi_1 + \cdots + \boldsymbol{d}_{n-1,m}\xi_m)] \end{aligned} \tag{59}$$

where $\boldsymbol{k}_i$ ($\bar{n} \times \bar{n}$ matrix) are all elements of control gain matrix K, i.e., $K = [\boldsymbol{k}_1, \boldsymbol{k}_2, \ldots, \boldsymbol{k}_n]$.

Then we have

$$\dot{\hat{\boldsymbol{x}}} = (A + BK)\hat{\boldsymbol{x}} + D(\boldsymbol{\Theta} + \hat{\boldsymbol{\Delta}}) \tag{60}$$

where

$$\boldsymbol{\Theta} = [\xi_1 \quad \xi_2 \quad \xi_3 \quad \cdots \quad \xi_m]^T \tag{61}$$

It is clear that the influence of the new disturbances $\hat{\boldsymbol{\Delta}}$ to the outputs can be completely eliminated if $\boldsymbol{\Theta} = -\hat{\boldsymbol{\Delta}}$, and the performance of the system can be determined by the control gain K.

Remark: For unmanned helicopter systems, the new disturbances $\hat{\boldsymbol{\Delta}}$ can be obtained through obtaining the external force disturbances $\bar{\boldsymbol{\Delta}}_F$ and moment disturbances $\bar{\boldsymbol{\Delta}}_M$ by using Eqs. (34), (28), (23), and (4). Furthermore, $\bar{\boldsymbol{\Delta}}_F$ and $\bar{\boldsymbol{\Delta}}_M$ can be easily obtained by using the linear and angular acceleration signals shown in the following equations:

$$\bar{\boldsymbol{\Delta}}_F = \ddot{\boldsymbol{p}} - [0 \quad 0 \quad g]^T - \frac{1}{m}R\boldsymbol{F}_c \bar{\boldsymbol{\Delta}}_M = \dot{\boldsymbol{\omega}} - I_b^{-1}(\boldsymbol{M}_c - \boldsymbol{\omega} \times I_b\boldsymbol{\omega}) \tag{62}$$

Since the high-order derivatives of the disturbance with respect to time are impossible to be measured or estimated, we cannot

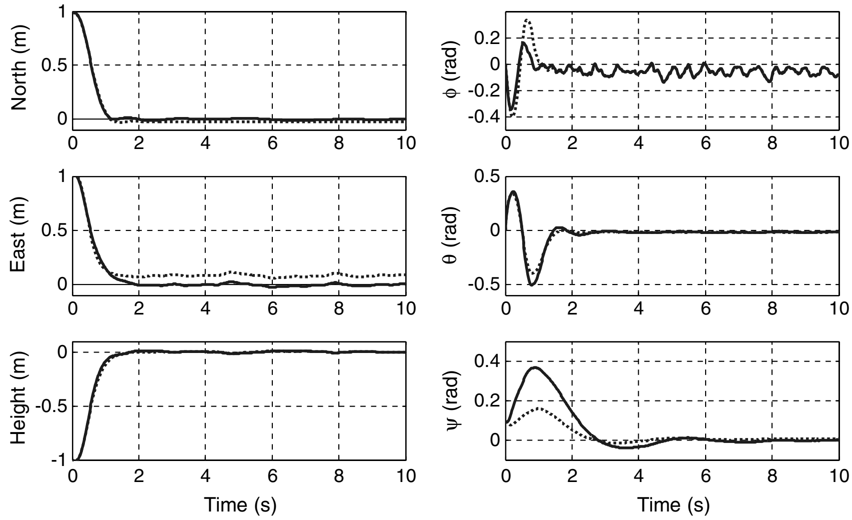

Fig. 5 Simulation results for model uncertainty rejection, where the solid line is for the AFC-enhanced H_∞ controller, and the dotted line is for the H_∞ controller.

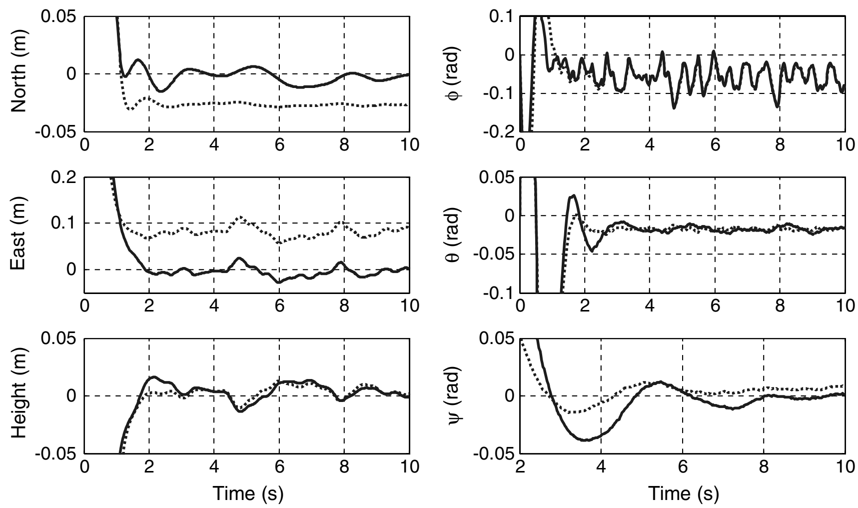

Fig. 6 Magnified version of Fig. 5.

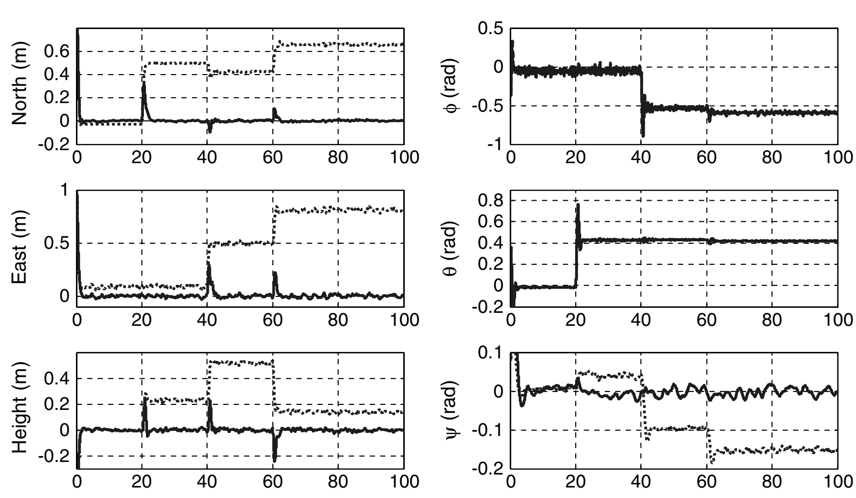

Fig. 7 Simulation results for both model uncertainty and external step-changed force, where the solid line is for the AFC-enhanced H_∞ controller, and the dotted line is for the H_∞ controller.

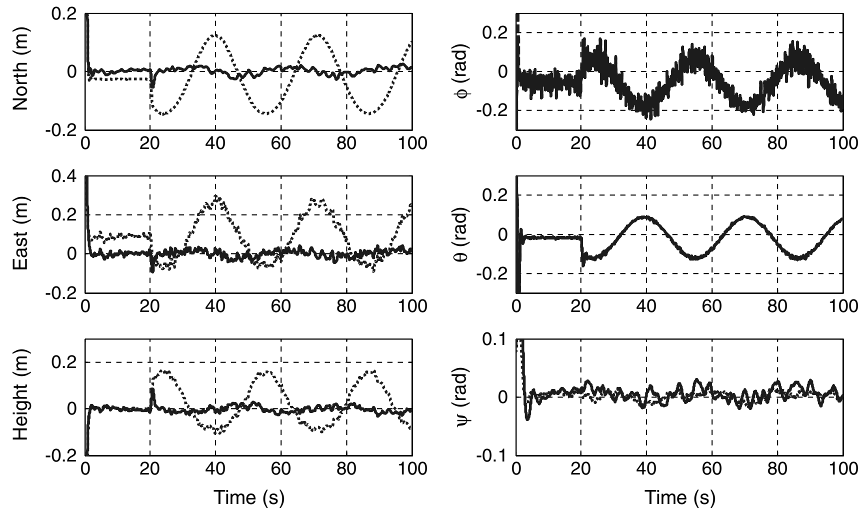

Fig. 8 Simulation results for both model uncertainty and external sin-changed force, where the solid line is for the AFC-enhanced H_∞ controller, and the dotted line is for the H_∞ controller.

completely eliminate the influence of disturbances on the outputs using this strategy.

Let $\mathbf{\Theta}$ satisfy the dynamical model

$$\mathbf{\Theta}^{(l)} + k_{l-1}\mathbf{\Theta}^{(l-1)} + \cdots + k_1\dot{\mathbf{\Theta}} + k_0\mathbf{\Theta} = k_l\mathbf{\Delta} \tag{63}$$

where $k_l, k_{l-1}, \ldots, k_1, k_0$ are some proper real numbers to be designed, and $l > n - 1$ is a positive integer.

By frequency domain analysis method, we have

$$\frac{(\mathbf{\Theta} + \mathbf{\Delta})(s)}{\mathbf{\Delta}(s)} = \frac{s^l + k_{l-1}s^{l-1} + \cdots + k_1 s + k_0 + k_l}{s^l + k_{l-1}s^{l-1} + \cdots + k_1 s + k_0} I \tag{64}$$

Equation (64) can be designed as a high-pass filter if 1) the denominator polynomial has no roots with positive real part, 2) $k_l + k_0 < k_0$, and 3) other parameters k_0, k_1, k_{l-1} are selected properly. Consequently, the low-frequency disturbance signals can be attenuated greatly.

This completes the controller design. The overall controller structure, which is referred to as an acceleration-feedback-enhanced H_∞ controller (or AFC-enhanced H_∞ controller), is described in Fig. 3. It is divided into four parts: 1) simplified inverse of aerodynamics, 2) feedback linearization, 3) nonlinear H_∞ controller, and 4) acceleration-feedback-enhanced controller. The simplified inverse of aerodynamics is realized by Eq. (31), where the controller output is the real input of the helicopter system a_{1s}, b_{1s}, θ_M, and θ_T, and the controller input is T_M^s and $\boldsymbol{M}^s$ computed by the feedback linearization method. Feedback linearization is used to transform the unmanned helicopter system's complicated nonlinear model into two linear models [Eq. (19)], where the controller output is used as the input of the simplified inverse aerodynamics controller, and the controller input $\boldsymbol{v}$ is the output of the nonlinear H_∞ controller. Subsequently, $\boldsymbol{v} = K\boldsymbol{x}$ in Theorem I is used as the H_∞ controller, which is robust with respect to the external disturbances and the uncertainties term $\boldsymbol{\delta}_1$ in Eq. (32) and takes outputs of acceleration feedback controller as inputs. Finally, Eq. (59) is the acceleration-feedback-enhanced controller through $\boldsymbol{v} = K\boldsymbol{x} + \tilde{\boldsymbol{v}}$.

Table 3 Tracking performance index E with respect to sine force disturbances

	H_∞ controller	AFC-enhanced H_∞ controller
Position, m	0.1872	0.0240
Yaw angle, rad	0.0066	0.0095

Remark: In general, we can design Eq. (63) separately for each ξ_i. If $\boldsymbol{d}_{1,i} = 0$, then $\xi_i^{(n-1)}$ will not appear in Eq. (59). Thus, it is not needed to design a linear filter with $l > n - 1$, which simplifies the design of Eq. (63).

V. Simulation

A series of simulations were conducted to verify the aforementioned AFC-enhanced H_∞ controller. Major parameters for a high-fidelity unmanned helicopter model are given in Table 1, and the simplified aerodynamics parameters required in Eq. (30) are given as

$$\begin{gathered} S_{L1} = -65.0398, \quad S_{L2} = -0.0620, \quad S_{M1} = 65.0398 \\ S_{M2} = -0.01, \quad S_{M3} = -1, \quad S_{N1} = -1, \quad S_{N2} = 0.8980 \\ S_{T_M1} = 1777, \quad S_{T_M2} = 39.8, \quad S_{T_T1} = 106.2, \quad S_{T_T2} = 6.9 \\ S_{Q_M1} = 95.6, \quad S_{Q_M2} = -1.8, \quad S_{Q_T1} = -3.9, \quad S_{Q_T2} = -0.03 \end{gathered} \tag{65}$$

The controller structure is shown in Fig. 3. The simplified inverse of aerodynamics and the feedback linearization control was designed using Eqs. (31) and (19), respectively. The H_∞ controller for position tracking error dynamics Eq. (32) and yaw angle tracking error dynamics Eq. (33) are

$$\begin{cases} \gamma_1 = 1 \\ \boldsymbol{v}_1 = K_1\boldsymbol{x} + \tilde{\boldsymbol{v}}_1 \\ K_1 = [-4173.8I_{3\times3} \quad -1980.8I_{3\times3} \quad -347.9I_{3\times3} \quad -24.2I_{3\times3}] \end{cases} \tag{66}$$

$$\begin{cases} \gamma_2 = 1 \\ \boldsymbol{v}_2 = K_2\boldsymbol{x} + \tilde{\boldsymbol{v}}_2 \\ K_2 = [-2.53 \quad -1.85] \end{cases} \tag{67}$$

Finally, the acceleration-feedback-enhanced controller $\tilde{\boldsymbol{v}}_1$ and $\tilde{v}_2$ is designed using Eqs. (59) and (63), and the parameters chosen are as follows:

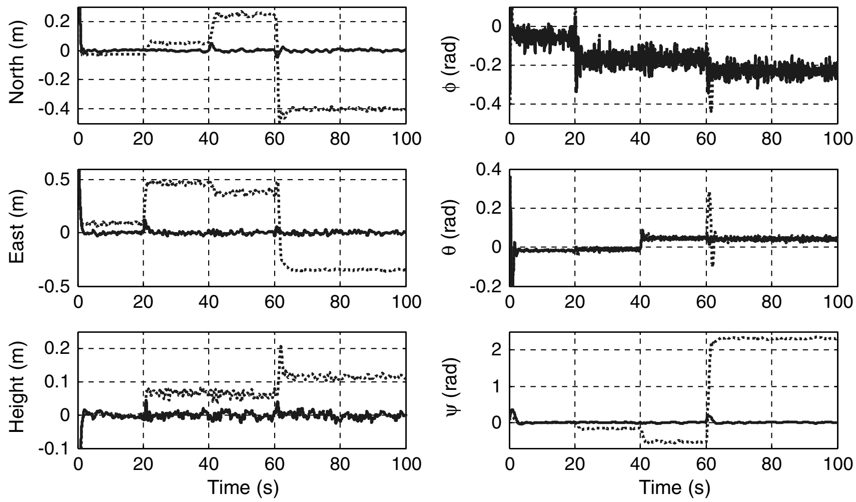

Fig. 9 Simulation result for both model uncertainty and external step-changed moment, where the solid line is for the AFC-enhanced H_∞ controller, and the dotted line is for the H_∞ controller.

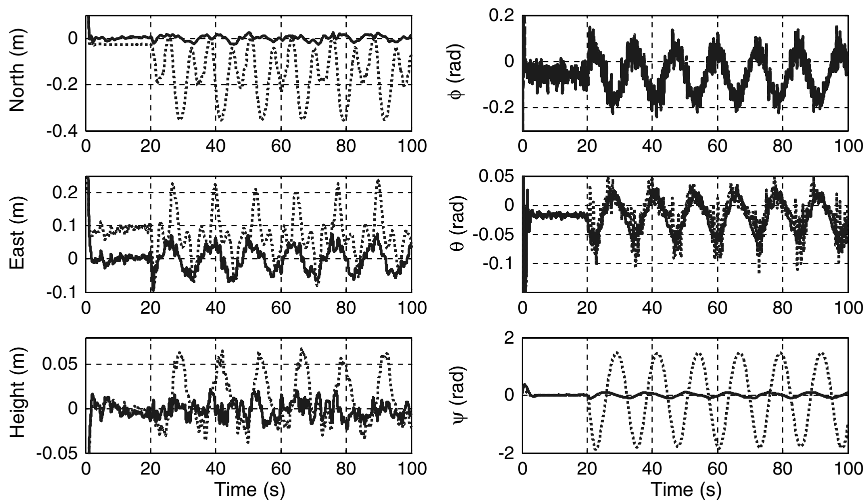

Fig. 10 Simulation result for both model uncertainty and external sin-changed moment, where the solid line is for the AFC-enhanced H_∞ controller, and the dotted line is for the H_∞ controller.

$$\begin{cases} \begin{bmatrix} \dddot{\xi}_1^1 \\ \dddot{\xi}_2^1 \\ \dddot{\xi}_3^1 \end{bmatrix} = -15 \begin{bmatrix} \ddot{\xi}_1^1 \\ \ddot{\xi}_2^1 \\ \ddot{\xi}_3^1 \end{bmatrix} - 75 \begin{bmatrix} \dot{\xi}_1^1 \\ \dot{\xi}_2^1 \\ \dot{\xi}_3^1 \end{bmatrix} - 125 \begin{bmatrix} \xi_1^1 \\ \xi_2^1 \\ \xi_3^1 \end{bmatrix} - 125\boldsymbol{\Delta}_1 \\ \begin{bmatrix} \dot{\xi}_4^1 \\ \dot{\xi}_5^1 \\ \dot{\xi}_6^1 \end{bmatrix} = -10 \begin{bmatrix} \xi_4^1 \\ \xi_5^1 \\ \xi_6^1 \end{bmatrix} - 10\boldsymbol{\Delta}_2 \\ \tilde{\boldsymbol{v}}_1 = \begin{bmatrix} \ddot{\xi}_1^1 \\ \ddot{\xi}_2^1 \\ \ddot{\xi}_3^1 \end{bmatrix} + \begin{bmatrix} \xi_4^1 \\ \xi_5^1 \\ \xi_6^1 \end{bmatrix} + 347.9 \begin{bmatrix} \xi_1^1 \\ \xi_2^1 \\ \xi_3^1 \end{bmatrix} + 24.2 \begin{bmatrix} \dot{\xi}_1^1 \\ \dot{\xi}_2^1 \\ \dot{\xi}_3^1 \end{bmatrix} \end{cases} \tag{68}$$

$$\begin{cases} \dot{\xi}_1^2 = -\xi_1^2 - 10\Delta_3 \\ \tilde{v}_2 = -\xi_1^2 \end{cases} \tag{69}$$

Table 4 Tracking performance index E, with respect to sine moment disturbances

	H_∞ controller	AFC-enhanced H_∞ controller
Position	0.1957	0.0355
Yaw angle	1.0444	0.0554

where Eq. (68) is for the position dynamics and Eq. (69) is for the yaw dynamics. The parameters of Eqs. (68) and (69) were chosen so that the cutoff frequency of Eq. (64) should be larger than the main frequency of disturbances.

Simulations were carried out to study a step-response, i.e., the helicopter was controlled to maneuver a step change from the initial states of $x_0 = y_0 = z_0 = 1.0$ m and $\Psi_0 = 0.1$ rad to a stabilized hover at $x = y = z = 0.0$ m and $\Psi = 0.0$ rad.

To demonstrate the performance of the proposed AFC-enhanced H_∞ controller, we compare its simulation results with the H_∞ controller, i.e., controller (66) and controller (67) without the terms $\tilde{\boldsymbol{v}}_1$ and $\tilde{v}_2$. To make the simulations as realistic as possible, we considered the real measurement/observation noise of accelerometers used in an unmanned helicopter. Figure 4 shows the linear accelerometers' measurement data for about 20 s during a flight experiment. The observational noise of the acceleration can be approximated by a Gaussian distribution with covariance of 0.0231. In all the simulations below, both the linear and angular acceleration signals were polluted by this noise. Five simulations were conducted, as listed in Table 2.

Figure 5 and its magnified version (Fig. 6) show the results of experiment 1, in which there is only the uncertainty due to the model simplification of Eq. (30). It can be seen that under the control of H_∞ controller (dashed line), the model uncertainty causes a stable tracking error that was eliminated successfully by the AFC-enhanced H_∞ controller (solid line).

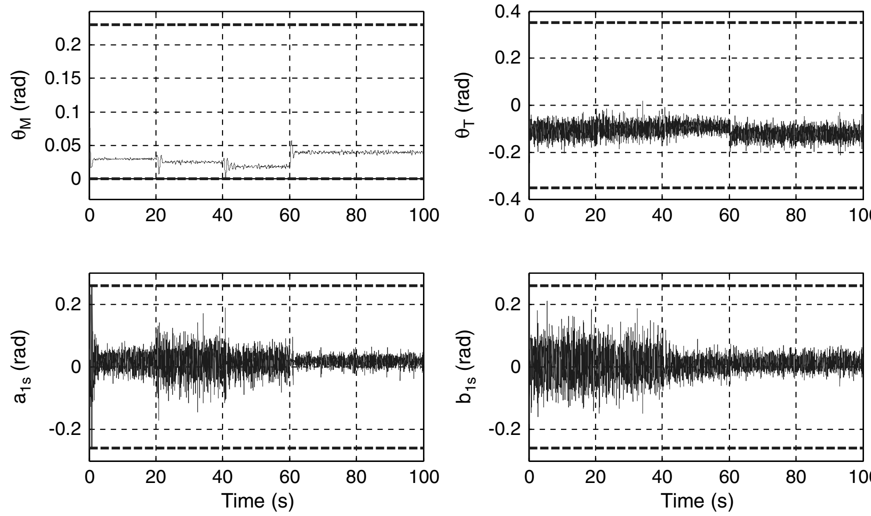

Fig. 11 Control inputs of AFC-enhanced H_∞ controller in experiment 2 (with step-changed force disturbances).

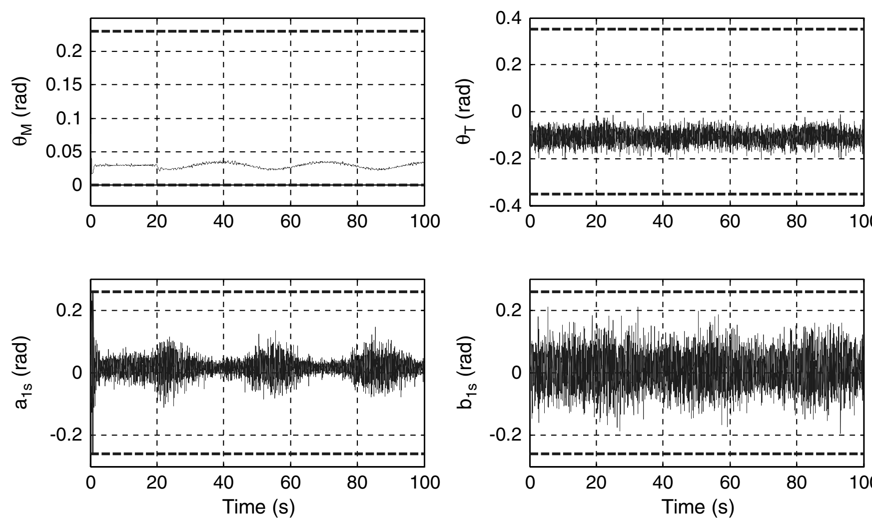

Fig. 12 Control inputs of AFC-enhanced H_∞ controller in experiment 3 (with sin-changed force disturbances).

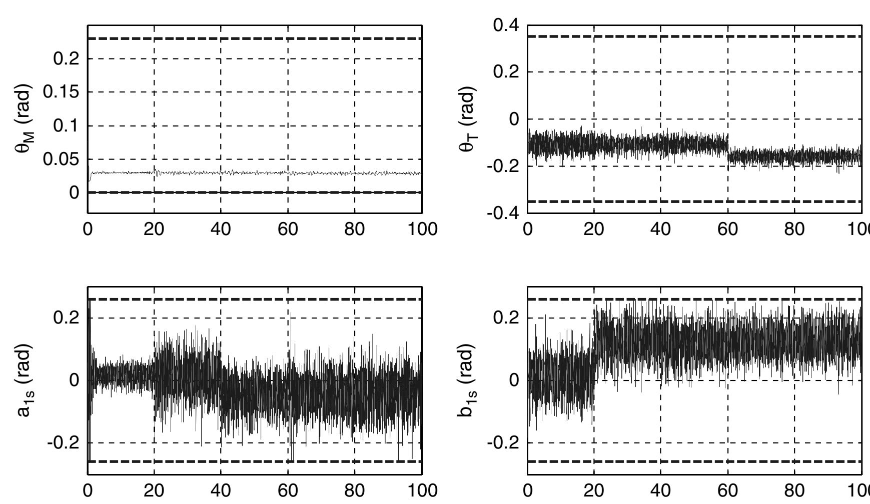

Fig. 13 Control inputs of AFC-enhanced H_∞ controller in experiment 4 (with step-changed moment disturbances).

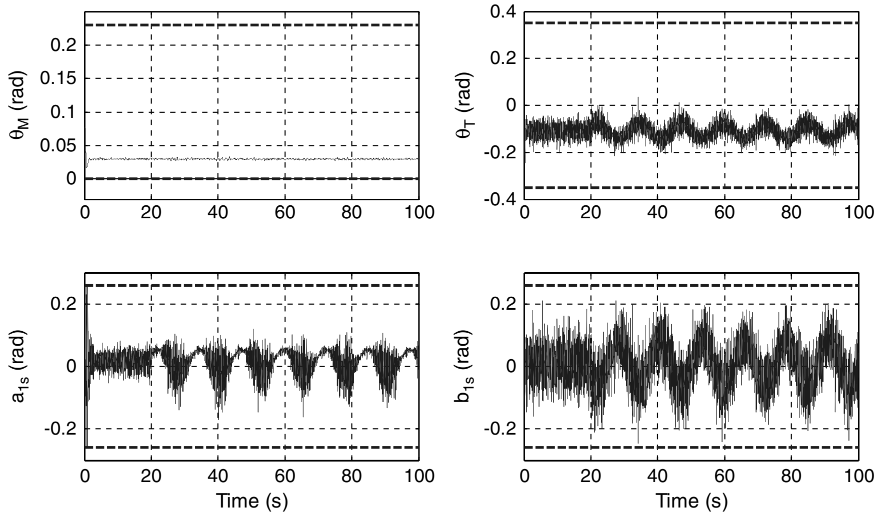

Fig. 14 Control inputs of AFC-enhanced H_∞ controller in experiment 5 (with sin-changed moment disturbances).

Figure 7 shows the results for experiment 2 in which external step force disturbances of 50 N occur suddenly to the system at every 20 s, i.e.,

$$\bar{\boldsymbol{\Delta}}_F = \begin{cases} [0\text{ N}, 0\text{ N}, 0\text{ N}]^T, & t < 20\text{ s} \\ [50\text{ N}, 0\text{ N}, 0\text{ N}]^T, & 20\text{ s} \le t < 40\text{ s} \\ [50\text{ N}, 50\text{ N}, 0\text{ N}]^T, & 40\text{ s} \le t < 60\text{ s} \\ [50\text{ N}, 50\text{ N}, 50\text{ N}]^T, & t \ge 60\text{ s} \end{cases} \tag{70}$$

It can be seen that the H_∞ controller cannot overcome the disturbance forces and there exist steady state position tracking errors that were rejected by the proposed AFC-enhanced H_∞ controller. It should be noted that both roll angle and pitch angle in this simulation are near 0.5 rad, which is reasonable, because to counteract the force disturbances, a body tilt is necessary for the main rotor to produce extra drag forces. In real helicopter systems, however, it would be dangerous for a helicopter system to stay at such a state.

Figure 8 is for experiment 3, in which external sine force disturbances of 10 N at $0.2\ \text{rad/s}$ are introduced to the system at 20 s, i.e.,

$$\bar{\boldsymbol{\Delta}}_F = \begin{cases} 0, & t < 20\text{ s} \\ 10\sin(0.2t) * [1, 1, 1]^T\ (\text{N}), & t \ge 20\text{ s} \end{cases} \tag{71}$$

It can be seen that the AFC-enhanced H_∞ controller attenuates the sine force disturbance better than the H_∞ controller. To quantify the performance improvement, an index function is introduced for evaluation of the tracking error:

$$E = \frac{1}{\text{num}} \sum_{i=1}^{\text{num}} \sqrt{[\boldsymbol{s}(t) - \boldsymbol{s}_d(t)]^T [\boldsymbol{s}(t) - \boldsymbol{s}_d(t)]} \tag{72}$$

where $\boldsymbol{s}(t)$ and $\boldsymbol{s}_d(t)$ are the interested position (yaw angle) and real position (yaw angle), respectively. The results are compared as listed in Table 3.

It can be seen that the AFC-enhanced H_∞ controller has a position tracking error that is about 6.8 times smaller than the H_∞ controller does and that both controllers have almost the same tracking error in yaw angle.

In addition to the force disturbance, the influence of moment disturbance on the closed-loop system was also simulated. The constant moment disturbance Eq. (73) was exerted on the helicopter model (i.e., experiment 4). Figure 9 show the results for this simulation in which the performance improvement can be found, similar to those controllers with constant force disturbance:

$$\bar{\boldsymbol{\Delta}}_M = \begin{cases} [0, 0, 0]^T\ \text{N}\cdot\text{m} & t < 20\text{ s} \\ [5, 0, 0]^T\ \text{N}\cdot\text{m}, & 20\text{ s} \le t < 40\text{ s} \\ [5, 5, 0]^T\ \text{N}\cdot\text{m}, & 40\text{ s} \le t < 60\text{ s} \\ [5, 5, 5]^T\ \text{N}\cdot\text{m}, & t \ge 60\text{ s} \end{cases} \tag{73}$$

In the last simulation, a sine moment disturbance below was given:

$$\bar{\boldsymbol{\Delta}}_M = \begin{cases} 0, & t < 20\text{ s} \\ 4 * \sin(0.5t) * [1, 1, 1]^T\ (\text{N}\cdot\text{m}), & t \ge 20\text{ s} \end{cases} \tag{74}$$

The results are shown in Fig. 10, in which the performance improvement is found similar to the case of sine force disturbances. The quantitative comparisons of the tracking errors using Eq. (72) are listed in Table 4.

From Table 4, it can be found that the AFC-enhanced H_∞ controller's position tracking error is 4.5 times smaller than that of the H_∞ controller; and the yaw angle tracking error is 17.8 times smaller than that of the H_∞ controller.

To simulate the effect of inputs saturation, we considered the following control input constraints:

$$a_{1s} \in [-0.26, 0.26]\text{ rad} \qquad b_{1s} \in [-0.26, 0.26]\text{ rad}$$
$$\theta_M \in [0, 0.23]\text{ rad} \quad \theta_T \in [-0.35, 0.35]\text{ rad} \tag{75}$$

Figures 11–14 show the performance of the AFC-enhanced H_∞ controller for the four simulation scenarios (Table 2) with the above control input saturation, respectively. There, the dashed line denotes the upper and lower boundaries of different control inputs. It can be found from these figures that the control input constrained by Eq. (75) is sufficient to attenuate the disturbances of Eqs. (70), (71), (73), and (74). If the disturbances are too large, however, the control inputs would become insufficient to fully alleviate the disturbance.

VI. Conclusions

In this paper, we presented an AFC-enhanced H_∞ controller and its design approach for a high-fidelity helicopter model. Our primary contribution is the generalization of the conventional AFC for use in systems (e.g. helicopter) involving nonlinear and underactuated characteristics. The other contribution is the use of the AFC to enhance the H_∞ controller by reducing its conservatism. Extensive simulations were performed with a helicopter model and two results are significant: the AFC-enhanced H_∞ controller can eliminate tracking errors under various uncertainties involved in the model parameters and external disturbances; and the AFC-enhanced H_∞ controller can attenuate the force and moment disturbances more effectively than an H_∞ controller.

References

[1] Shim, H., Koo, T. J., Hoffmann, F., and Sastry, S., "A Comprehensive Study of Control Design for an Autonomous Helicopter," *Proceedings of the 37th IEEE Conference on Decision and Control*, Inst. of Electrical and Electronics Engineers, Piscataway, NJ, 1998, pp. 3653–3658.
doi:10.1109/CDC.1998.761749

[2] Cai, G. W., Chen, B. M., Kemao, P., Miaobo, D., and Lee, T. H., "Modeling and Control of the Yaw Channel of a UAV Helicopter," *IEEE Transactions on Industrial Electronics*, Vol. 55, No. 9, 2008, pp. 3426–3434.
doi:10.1109/TIE.2008.926780

[3] Frazzoli, E., Dahleh, M. A., and Feron, E., "Trajectory Tracking Control Design for Autonomous Helicopters Using a Backstepping Algorithm," *Proceedings of the 2000 American Control Conference*, Inst. of Electrical and Electronics Engineers, Piscataway, NJ, 2000, pp. 4102–4107.
doi:10.1109/ACC.2000.876993

[4] Shim, H., "Hierarchical Flight Control System Synthesis for Rotorcraft-Based Unmanned Aerial Vehicles," Ph.D. Dissertation, Mechanical Engineering Department, Univ. of California, Berkeley, Berkeley, CA, 2000, pp. 18–65.

[5] Bogdanov, A., Carlsson, M., Harvey, G., Hunt, J., Kieburtz, R., Van der Merwe, R., and Wan, E., "State-Dependent Riccati Equation Control of a Small Unmanned Helicopter," AIAA Guidance, Navigation, and Control Conference and Exhibit, AIAA Paper 2003-5672, Austin, TX, Aug. 2003.

[6] Raffo, G. V., Ortega, M. G., and Rubio, F. R., "Backtepping/Nonlinear H_∞ Control for Path Tracking of a Quadrotor Unmanned Aerial Vehicle," *Proceedings of 2008 American Control Conference*, Inst. of Electrical and Electronics Engineers, Piscataway, NJ, June 2008, pp. 3356–3361.
doi:10.1109/ACC.2008.4587010

[7] Bogdanov, A., Wan, E. A., Carlsson, M., Zhang, Y., Kieburtz, R., and Baptista, A., "Model Predictive Neural Control of a High-Fidelity Helicopter Model," AIAA Guidance, Navigation and Control Conference and Exhibit, AIAA Paper 2001-4164, Montreal, Aug. 2001.

[8] Brunke, S., and Campbell, M., "Estimation Architecture for Future Autonomous Vehicles," *Proceedings of the 2002 American Control Conference*, Inst. of Electrical and Electronics Engineers, Piscataway, NJ, May 2002, pp. 1108–1114.
doi:10.1109/ACC.2002.1023167

[9] Yang, C. D., and Kung, C. C., "Nonlinear H infinity Flight Control of General Six Degree-of-Freedom Motions," *Journal of Guidance, Control, and Dynamics*, Vol. 23, No. 2, 2000, pp. 278–288.
doi:10.2514/2.4520

[10] Takahashi, M. D., "H_∞ Helicopter Flight Control Law Design with and Without Rotor State Feedback," *Journal of Guidance, Control, and Dynamics*, Vol. 17, No. 6, Nov.–Dec., 1994, pp. 1245–1251.
doi:10.2514/3.21340

[11] Han, J. D., He, Y. Q., and Xu, W. L., "Angular Acceleration Estimation and Feedback Control: An Experimental Investigation," *Mechatronics*, Vol. 17, No. 9, Oct. 2007, pp. 524–532.
doi:10.1016/j.mechatronics.2007.05.006

[12] Xu, W. L., Han, J. D., and Tso, S. K., "Experimental Study of Contact Transition Control Incorporating Joint Acceleration Feedback," *IEEE/ASME Transactions on Mechatronics*, Vol. 5, No. 3, Sept. 2000, pp. 292–301.
doi:10.1109/3516.868921

[13] Han, J. D., Wang, Y. C., Tan, D. L., and Xu, W. L., "Acceleration Feedback Control for Direct-Drive Motor System," *Proceedings of IEEE International Conference on Intelligent Robots and Systems*, Vol. 2, Inst. of Electrical and Electronics Engineers, Piscataway, NJ, 2000, pp. 1068–1074.
doi:10.1109/IROS.2000.893161

[14] Mizuochi, M., Tsuji, T., and Ohnishi, K., "Multirate Sampling Method for Acceleration Control System," *IEEE Transactions on Industrial Electronics*, Vol. 54, No. 3, 2007, pp. 1462–1471.
doi:10.1109/TIE.2007.893002

[15] Tomikawa, Y., and Okada, S., "Piezoelectric Angular Acceleration Sensor," *2003 IEEE Symposium on Ultrasonics*, Vol. 2, Inst. of Electrical and Electronics Engineers, Piscataway, NJ, Oct. 2003, pp. 1346–1349.
doi:10.1109/ULTSYM.2003.1293152

[16] Xion, Y. H., Ma, B. H., and Peng, X. P., "Measurement of Angular and Linear Accelerations Using Linear Accelerometers," *Journal of Beijing Institute of Technology*, Vol. 9, No. 3, 2000, pp. 307–311.

[17] Qi, J. T., Song, D. L., Dai, L., and Han, J. D., "The ServoHeli-20 Rotorcraft UAV Project," *15th International Conference on Mechatronics and Machine Vision in Practice (M2VIP08)*, Inst. of Electrical and Electronics Engineers, Piscataway, NJ, Dec. 2008, pp. 92–96.
doi:10.1109/MMVIP.2008.4749513

[18] Koo, T. J., and Sastry, S., "Output Tracking Control Design of a Helicopter Model Based on Approximate Linearization," *Proceedings of the 37th IEEE Conference on Decision & Control*, Vol. 4, Inst. of Electrical and Electronics Engineers, Piscataway, NJ, Dec. 1998, pp. 3635–3640.
doi:10.1109/CDC.1998.761745

[19] Doyle, J. C., Glover, K., Khargonekar, P. P., and Francis, B. A., "A State-Space Solutions to Standard H_2 and H_∞ Control Problems," *IEEE Transactions on Automatic Control*, Vol. 34, No. 8, Aug. 1989, pp. 831–847.
doi:10.1109/9.29425